

Elsevier Editorial System(tm) for Quaternary Research
Manuscript Draft

Manuscript Number: YQRES-D-15-00014R2

Title: Climate changes, metal pollution and soil erosion in South Greenland over the past 700 years

Article Type: Research Paper

Keywords: Greenland; Norse; soil erosion; Little Ice Age; lead (Pb); metal pollution; FTIR; pollen; geochemistry

Corresponding Author: Ms. Noemí Silva-Sánchez, Msc

Corresponding Author's Institution: Universidad de Santiago de Compostela

First Author: Noemí Silva-Sánchez, Msc

Order of Authors: Noemí Silva-Sánchez, Msc; J. Edward Schofield, Dr.; Tim M. Mighall, Dr. ; Antonio Martínez Cortizas, Professor; Kevin J. Edwards, Professor; Ian Foster, Professor

Abstract: A peat core from southern Greenland provided a rare opportunity to investigate human-environment interactions, climate change and atmospheric pollution over the last ~700 cal years. X-ray fluorescence, gas chromatography-combustion, isotope ratio mass spectrometry, peat humification and fourier-transform infrared spectroscopy were applied and combined with palynological and archaeological evidence. Variations in peat mineral content seem to be related to soil erosion linked with human activity during the late Norse period (13th-14th centuries AD) and the modern era (20th century). Cooler conditions during the Little Ice Age (LIA) are reflected by both slow rates of peat growth and carbon accumulation, and by low bromine (Br) concentrations. Spörer and Maunder minima in solar activity may be indicated by further declines in Br and enrichment in easily-degradable compounds such as polysaccharides. Peat organic matter composition was also influenced by vegetation changes at the end of the LIA when the expansion of oceanic heath was associated with polysaccharide enrichment. Atmospheric lead pollution was recorded in the peat after AD 1845, and peak values occurred in the 1970s. There is indirect support for a predominantly North American lead source, but further Pb isotopic analysis would be needed to confirm this hypothesis.

1 **Climate changes, lead pollution and soil erosion in South Greenland**
2 **over the past 700 years**

3

4 **Noemí Silva-Sánchez*^a, J. Edward Schofield^b, Tim M. Mighall^b, Antonio Martínez**
5 **Cortizas^a, Kevin J. Edwards^{b,c}, Ian Foster^d**

6

7 ^a Edafología y Química Agrícola, Fac. Biología, Campus Sur, Universidad de Santiago de
8 Compostela, Rúa Lope Gómez de Marzoa s/n. E-15782, Spain

9

10 ^b Department of Geography & Environment, School of Geosciences, University of Aberdeen,
11 Elphinstone Road, Aberdeen AB24 3UF, UK

12

13 ^c Department of Archaeology, School of Geosciences, University of Aberdeen, Elphinstone
14 Road, Aberdeen AB24 3UF, UK

15

16 ^d School of Science and Technology, University of Northampton, Newton Building,
17 Northampton NN2 6JD, UK

18

19

20

21

22 *Corresponding author:

23 noemi.silva.sanchez@usc.es, n.o.e.s@hotmail.com

24 Tel. +34 881813315

25 **Abstract**

26

27 A peat core from southern Greenland provided a rare opportunity to investigate human-
28 environment interactions, climate change and atmospheric pollution over the last ~700 cal
29 years. X-ray fluorescence, gas chromatography-combustion, isotope ratio mass spectrometry,
30 peat humification and fourier-transform infrared spectroscopy were applied and combined
31 with palynological and archaeological evidence. Variations in peat mineral content seem to
32 be related to soil erosion linked with human activity during the late Norse period (13th-14th
33 centuries AD) and the modern era (20th century). Cooler conditions during the Little Ice Age
34 (LIA) are reflected by both slow rates of peat growth and carbon accumulation, and by low
35 bromine (Br) concentrations. Spörer and Maunder minima in solar activity may be indicated
36 by further declines in Br and enrichment in easily-degradable compounds such as
37 polysaccharides. Peat organic matter composition was also influenced by vegetation changes
38 at the end of the LIA when the expansion of oceanic heath was associated with
39 polysaccharide enrichment. Atmospheric lead pollution was recorded in the peat after ~AD
40 1845, and peak values occurred in the 1970s. There is indirect support for a predominantly
41 North American lead source, but further Pb isotopic analysis would be needed to confirm this
42 hypothesis.

43

44 **Keywords:** Greenland, Norse, soil erosion, Little Ice Age, lead (Pb), metal pollution, FTIR,
45 pollen, geochemistry

46

47

48

49

50 **Introduction**

51

52 Ombrotrophic peatlands, receiving their inputs (precipitation and dusts) solely from the
53 atmosphere, are widely recognised as important environmental archives. The stratified
54 records of chemical elements and biological proxies contained within raised mires and
55 blanket bogs can be used, for example, to provide information about changes in climate or
56 land use, and levels of atmospheric pollution, during prehistory through to post-industrial
57 times (e.g. Chambers et al., 2012; Meharg et al., 2012; Martínez Cortizas et al., 2013;
58 Pontevedra-Pombal et al., 2013). Peat geochemical studies are available for locations across
59 the major continental land masses and peripheries of North America and Western Europe, yet
60 relatively few Holocene records exist from mid to high latitude North Atlantic islands.
61 Evidence from Greenland, Iceland and the Faroes would enhance spatial data coverage for
62 sites influenced by related atmospheric systems. The North Atlantic islands have relatively
63 short and frequently interrupted histories of human occupation, with continuous recent
64 (European) settlement dating back only to Norse colonisation (*landnám*) during the period
65 ~AD 800-1000 (Fitzhugh and Ward, 2000). Where environmental archives of sufficient
66 continuity and antiquity present themselves, these potentially offer opportunities to establish
67 a geochemical baseline for 'pristine' North Atlantic environments during periods when
68 people were absent from the landscape (cf. Dugmore et al., 2005).

69

70 Few peat geochemical investigations have been conducted in Greenland (Fig. 1a). Apart from
71 cost and logistics, this is because peatlands are not extensive and raised bogs are absent
72 (Feilberg, 1984). Some data are available from minerotrophic, groundwater-fed fens which
73 demonstrate that such wetlands may preserve a record of atmospheric deposition, even
74 though the identification of regional atmospheric signals can be complicated by mineral

75 inputs from local sources (e.g. slopewash). Shotyk et al. (2003) used a fen developed between
76 two small lakes near Tasiusaq (Fig. 1b), southern Greenland, to reconstruct fluxes of selected
77 elements, notably mercury (Hg), lead (Pb) and arsenic (As), and related these to atmospheric
78 deposition of anthropogenic origins after ~AD 1950. Their profile extended back ~2500 cal
79 yr BP, but at reduced temporal resolution through the older part of the sequence. Schofield et
80 al. (2010) presented a geochemical record from the nearby site of Qinngua (Fig. 1b),
81 concentrating on the behaviour of lithogenic elements and halogens, and linking this to
82 patterns of soil erosion and storminess over the last *ca* 1000 cal yr, albeit noting a significant
83 hiatus in the profile (~AD 1380-1950).

84

85 An investigation by Golding et al. (2011) at the Norse farmstead of Sandhavn (Fig. 1b), near
86 the southern tip of Greenland, revealed a small peat-filled depression set within a rock
87 platform (Figs 1c and 1d). The basin appears isolated from the groundwater table and
88 radiometric dating indicates that peat growth has apparently been continuous since the mid-
89 13th century AD. This provided a rare opportunity to characterise the geochemical signal
90 contained within a predominantly rain-fed peat from a Greenlandic setting. The main
91 objectives of the research reported here are: (i) to search for geochemical signatures that are
92 representative of changes in climate and of possible impacts arising from past human activity
93 at the site (e.g. soil erosion); (ii) to study the relationship between climate, vegetation and
94 peat decomposition in a subarctic environment; (iii) to establish high resolution records for
95 atmospheric metal pollution and to discuss likely sources for these. Although the peat profile
96 from Sandhavn spans a relatively short timeframe (~AD 1250-2000) and cannot provide
97 baseline environmental information for the period before the arrival of Norse settlers, the
98 research is important because: (a) it provides data encompassing a significant climatic
99 perturbation – the Little Ice Age (LIA; Grove, 1988); (b) the basin is adjacent to the

100 homefields (i.e. the hay-producing areas) of a Norse farmstead (Fig. 1d) that was in use from
101 ~AD 1000-1400, and the sampling location was anticipated to be particularly sensitive to the
102 environmental impacts arising during the past human occupation and use of the site; (c) the
103 results presented on peat decomposition may prove informative for studies with a focus on
104 long-term carbon sequestration by peatlands.

105

106 **Site background and context**

107

108 Sandhavn (59°59'N, 44°46'W; Fig. 1) is located on the Ikigait peninsula on the outer coast of
109 Greenland, approximately 50 km northwest of Cape Farewell (the most southerly point in
110 Greenland). The prevailing climate is subarctic, with cold winters and cool summers and a
111 notable feature of the climate regime is frequent strong winds. The seas here are regarded as
112 the windiest in the world ocean with speeds exceeding 20 ms⁻¹ (equivalent to a strong gale)
113 around 20% of the time (Sampe and Shang-Ping, 2007). Wind direction is bimodal, with a
114 strong probability of observing both westerly and easterly high speed wind events (Moore et
115 al., 2008; Renfrew et al., 2008), which might have implications for the sourcing of
116 atmospheric dusts deposited across the area.

117

118 The solid geology of south Greenland comprises granites and gneisses of the Ketilidian
119 mobile belt, with basic and intermediate intrusions (Allaart, 1976). This creates a rugged
120 alpine topography characterised by steep slopes and peaks sometimes exceeding 1000 m a.s.l.
121 The soils can be broadly classified as cryosols, with many showing evidence for
122 podsolization (Golding et al., 2011). *Empetrum nigrum* (crowberry) oceanic heath is the
123 dominant vegetation in the coastal zone. This is replaced by more subcontinental plant
124 communities – primarily *Betula-Salix* (birch-willow) dwarf heath – within the warmer and

125 drier interior (Böcher et al., 1968; Feilberg, 1984). The basin featured in this investigation
126 (Fig. 1c) supports nutrient-poor mire dominated by sedges (*Carex rariflora* and *C. bigelowii*),
127 interspersed with small pools fringed by mare's-tail (*Hippuris vulgaris*). There are no
128 inflowing streams entering the basin, which is set within a rock outcrop that is elevated
129 slightly above the general level of the land around it (Fig. 1d). Consequently any minerogenic
130 inputs reaching the basin via runoff from the surrounding area will have been restricted to an
131 extremely localised radius (~10-20 m) defined by the rocky rim around the basin. Thus,
132 whilst the setting cannot be defined as strictly ombrotrophic, the majority of inputs to the
133 basin must come from the atmosphere. This supposition is further supported by high organic
134 LOI values, high C contents and low concentrations of lithogenic elements in the peat
135 (discussed below).

136

137 The ruins of a Viking/Norse farmstead and Thule Inuit dwellings can be found at Sandhavn.
138 These, together with landscape, soils and pollen-based evidence from the site (Raahauge et
139 al., 2003; Golding et al., 2011, 2014) attest to a local human presence between ~AD 1000-
140 1400, i.e. throughout most of the period conventionally ascribed to the occupation of the
141 Norse Eastern Settlement of Greenland (Krogh, 1967). The neighbouring farm and port of
142 Herjolfsnes, ~3.5 km east-southeast of Sandhavn, was perhaps in use until slightly later (~AD
143 1450) before also being abandoned (Arneborg et al., 1999). The Royal Greenlandic Trading
144 Company had a trading station here from AD 1834-1877. Sheep farming occurred briefly on
145 the Ikigait peninsula from 1959-1972 (Arneborg, 2006), although pastoral agriculture has
146 been in continuous operation more widely across southern Greenland since 1924 (Fredskild,
147 1988). The area immediately around Sandhavn has otherwise been uninhabited, with the
148 possible exception of occasional Thule maritime hunters whose impact on the landscape
149 would probably have been negligible.

150

151 **Methods**

152

153 *Fieldwork*

154

155 In August 2008, a short (40cm) peat monolith was recovered from a small (~30 m diameter)
156 basin (59°59.875'N, 44°46.637'W) adjacent to the former homefields and Norse ruins at
157 Sandhavn (Fig. 1c). Samples were collected by inserting a monolith tin into the open face of a
158 pit dug into the mire. The field stratigraphy comprised a base of saturated coarse grey-brown
159 sands overlain by ~36 cm of orange-brown *turfa* (rootlet) peat containing abundant
160 bryophytes. The peat was visibly darker above 17 cm. The top of the profile (5-0 cm)
161 contained the (living) root mat. The monolith was wrapped in polythene and returned to the
162 University of Aberdeen, where it was kept refrigerated (4 °C) prior to sub-sampling in the
163 laboratory.

164

165 *Radiocarbon dating and age-modelling*

166

167 Four AMS (accelerator mass spectrometry) ¹⁴C measurements were taken on bryophytes
168 selected from the peat (Table 1). These were first reported in Golding et al. (2011) where they
169 were used to produce an age-depth model based upon a polynomial fitted through the median
170 probabilities of the calibrated radiocarbon dates. The addition of ²¹⁰Pb-dating to the profile
171 (as outlined below) and developments in software now allow an improved age-depth model
172 to be produced. The revised model uses 'classical' age-depth modelling (*Clam*; Blaauw,
173 2010) to apply a smoothed spline through the dates. The 'best estimates' from this model

174 have been used to provide calendar dates for events in the geochemical and biological records
175 through the organic (peat) section of the profile.

176

177 *²¹⁰Pb-dating*

178

179 The unsupported ²¹⁰Pb_{un} activity within samples towards the peat surface was ascertained by
180 subtraction of the supported component (measured as ²¹⁴Pb at 295.22 and 351.93 keV) from
181 the total ²¹⁰Pb activity measured at 46.54 keV (Wallbrink et al., 2002). ²¹⁰Pb and ²¹⁴Pb
182 activities were measured using EG&G ORTEC hyper-pure Germanium detectors in a well
183 configuration (11 mm diameter, 40 mm depth) housed at Coventry University. The method
184 for calculating the age-depth relationship follows procedures described by Appleby and
185 Oldfield (1978), Appleby (2001) and Walling et al. (2002). Accumulation rates varied down
186 core and the CRS dating model was used to calculate ages (Appleby et al., 1988; Appleby,
187 2001).

188

189 *Pollen analysis*

190

191 Full details of the methods are described in Golding et al. (2011). Pollen samples were
192 prepared using NaOH, HF and acetolysis techniques with samples embedded in silicone oil of
193 12,500 cSt viscosity (Moore et al., 1991). Palynomorphs were counted until a sum in excess
194 of 500 TLP (total land pollen, excluding aquatics and spores) was achieved. Percentage data
195 were calculated using TILIA (Grimm, 1992) and the pollen diagram of selected taxa
196 constructed using TGView (Grimm, 2004). Coprophilous fungal spores (van Geel et al.,
197 2003) were also counted and these are expressed as a percentage of the TLP sum. These

198 spores are given the type numbers assigned by the Hugo de Vries-Laboratory, Amsterdam,
199 and are prefixed *HdV*-.

200

201 *Loss-on-ignition (LOI) and Dry Bulk Density*

202

203 The organic content of samples was measured through LOI. This was calculated following
204 the combustion of dried and milled samples in a muffle furnace for 3 hours at 550 °C. Dry
205 weights were also used to calculate dry bulk density of the peat which, in turn, allowed the
206 determination of peat carbon accumulation rates (PCAR).

207

208 *Elemental analysis and isotopic ratio mass spectroscopy*

209

210 Laboratory sub-sampling for elemental analysis was done at 1 cm contiguous intervals. Prior
211 to measurement, samples were dried and milled to a fine powder with an agate mill.

212 Concentrations of major and minor elements (Si, Al, Fe, Ti, Ca, K, P and S), trace lithogenic
213 elements (Rb, Sr, Zr, Nb, Y, Ga), trace metallic elements (Mn, Cr, Ni, Cu, Zn and Pb),

214 halogens (Cl and Br) and selenium (Se) were determined by X-ray fluorescence (XRF) using

215 an EMMA-XRF (Cheburkin and Shotykh, 1996) hosted at the XRD-XRF facility of RIAIDT

216 (Red de Infraestructuras de Apoyo a la Investigación y al Desarrollo Tecnológico) at the

217 University of Santiago de Compostela. Peat and mineral samples were calibrated using a

218 calibration for organic and inorganic matrices respectively. Detection limits (DL) were as

219 follows: Si (0.05%), Ti and Fe (0.002%), Al (0.002% for organic; 0.2% for inorganic

220 matrices), Ca (0.002%; 0.01%), K (0.002%; 0.05%), P (0.009%; 0.03%), S (0.009%; 0.03%),

221 Rb ($0.5 \mu\text{g g}^{-1}$; $5 \mu\text{g g}^{-1}$), Sr ($0.5 \mu\text{g g}^{-1}$; $5 \mu\text{g g}^{-1}$), Mn ($5 \mu\text{g g}^{-1}$; $30 \mu\text{g g}^{-1}$), Pb ($0.5 \mu\text{g g}^{-1}$), Se

222 ($0.5 \mu\text{g g}^{-1}$; $2 \mu\text{g g}^{-1}$), Br ($0.5 \mu\text{g g}^{-1}$; $2 \mu\text{g g}^{-1}$) and Cl ($40 \mu\text{g g}^{-1}$; $350 \mu\text{g g}^{-1}$). Calibrations for Zr

223 were not provided, thus we used normalized intensities with z-score transformation for
224 comparison with other elements.

225

226 The elemental analyses of C and N, and the $\delta^{13}\text{C}$ and $\delta^{15}\text{N}$ isotopic ratio analyses, were
227 carried out using a gas chromatography-combustion elemental analyser (GC/C; EA1108
228 CarboErba Instruments) coupled by a Conflowll interphase (ThermoFinnigan) with an
229 isotope ratio mass spectrometer (IRMS; MAT253 ThermoFinnigan). Sample isotopic
230 composition is expressed as units of $\delta^{13}\text{C}$ and $\delta^{15}\text{N}$ using Pee Dee Belemnite (PDB) and air
231 atmosphere as the standards for C and N respectively.

232

233 *Fourier Transform Infrared Spectroscopy (FTIR)*

234

235 Spectral characterization of peat samples was made in the IR-RAMAN unit of RIAIDT, and
236 performed by FTIR spectroscopy using a Bruker IFS-66V FTIR spectrometer. The resolution
237 was set to 4 cm^{-1} and 32 scans per sample were recorded. The operating range was 400-4000
238 cm^{-1} . One mg of homogenised (milled) sample was mixed thoroughly with 100 mg of KBr
239 (FTIR grade) and a pellet was prepared using a press. To avoid differences in absorbance
240 related to sample preparation and detection, various procedures were applied to transform the
241 baseline corrected spectra (Solomon et al., 2007; Smidt et al., 2008). The main FTIR bands
242 used in this study and their meaning are shown in Table SI1.

243

244 *Degree of peat humification (DPH)*

245

246 Peat humification was measured following the method of extracting humic acids from dried
247 and milled peat samples using 8% NaOH and assessing the concentrations of solutions

248 colorimetrically using a spectrophotometer (Blackford and Chambers, 1993). Results are
249 expressed as percentage transmittance.

250

251 *Statistics*

252

253 The use of multivariate statistical approaches helps to summarize common patterns of
254 variation within datasets and to gain insights into the underlying environmental factors that
255 control these. For elemental composition data and LOI (collectively PCe), and organic matter
256 properties – FTIR, C/N, $\delta^{13}\text{C}$, $\delta^{15}\text{N}$ and DPH – (collectively PCo), principal components
257 analyses (PCA) were applied using SPSS 20 in correlation mode and by applying a varimax
258 rotation. Prior to analysis, the dataset was standardized using z-scores (Eriksson et al., 1999).

259

260 **Results and interpretation**

261

262 *Chronology*

263

264 Radiocarbon dates are shown in Table 1 and an age-depth model for the profile is presented
265 in Figure 2. This pertains to the organic part of the sequence; the basal sands, which are of
266 unknown age, were not considered. The model shows that the peat accumulation rate has
267 varied considerably over the last ~750 cal yr. The rate was initially very low, ~0.025-0.033
268 cm yr^{-1} from ~AD 1250-1400 (equivalent to a deposition time [DT] of ~30-40 yr cm^{-1}). The
269 rate of peat growth reduced further during the period *ca* AD 1400-1800 (~0.020-0.025 cm yr^{-1} ;
270 DT ~40-50 yr cm^{-1}). The accumulation of organic matter accelerated rapidly during the last
271 two centuries, especially during the second half of the 20th century when peat accumulation

272 increased to $\sim 0.2 \text{ cm yr}^{-1}$ ($DT \sim 5 \text{ yr cm}^{-1}$). This pattern translates into a low temporal
273 resolution for the bottom half of the peat monolith, but a highly resolved archive above this.

274

275 *Pollen analysis*

276

277 Full details of the pollen analysis have already been presented in Golding et al. (2011).

278 Selected taxa appropriate to the discussion of the new geochemical data are presented in
279 Figure 3.

280

281 *Elemental composition and LOI*

282

283 The transition from basal sand to peat (36-35 cm) is the key stratigraphic change in the
284 monolith. This is reflected by sharp differences in LOI and element concentrations across the
285 sediment contact (Fig. SI.1). In order to optimise the visibility of changes through the peat
286 section (Fig. 4), PCA was applied only to those samples above the transition (Fig. 5). Three
287 principal components (PCe), which explain 77.1% of the total variance, were extracted
288 (Table SI2).

289

290 The first principal component (PC1e) explains 38.9% of the variance. Most lithogenic
291 elements and some trace metals (Ti, Si, Zr, Al and Rb), together with N, P and S, show high
292 positive loadings for PC1e, whilst LOI displays a large negative loading. The record of factor
293 scores can be divided into three main sections. From 35-32 cm the scores are positive but
294 decreasing; from 32-16 cm the scores fluctuate between small negative and positive values;
295 and the scores decrease steadily to large negative values from 16 cm to the surface. The large

296 contribution of lithogenic elements and their opposition with LOI indicate that this
297 component mainly reflects the mineral content of the peat.

298

299 The second principal component (PC2e) explains 20.2% of the variance. Iron, Br, Pb and Cl
300 have high positive loadings for PC2e whilst S shows a moderate negative loading. Factor
301 scores for PC2e (Fig. 5) are negative except for a broad peak from 22-9 cm. Iron
302 accumulation in peat is largely controlled by redox conditions (Chesworth et al., 2006), with
303 the concentration of Fe increasing under oxidisation (e.g. during water table drawdown). The
304 halogens (Br and Cl) are likely to be of marine origin and are mostly preserved in peat as
305 organohalogenated compounds formed by oxygen-dependent enzymatic processes. Thus,
306 their concentrations in peat, although also dependent on atmospheric fluxes, are mainly
307 controlled by biotic halogenation and dehalogenation (Myneni, 2002; Biester et al., 2004;
308 Leri and Myneni, 2012). Lead may have both geogenic and pollution sources, but its increase
309 here seems to be linked to atmospheric pollution as it does not have a strong association with
310 the major and minor lithogenic elements.

311

312 The third principal component (PC3e) explains 18% of the variance and is most strongly
313 related to K, Mn, Ca (high positive loadings), and to a lesser extent Sr (moderate positive
314 loadings) and C (moderate negative loadings). PC3e scores show a similar record to PC1e
315 scores below 16 cm, suggesting that in this peat section, K, Mn and Ca are mainly of
316 geogenic origin. Contrary to PC1e, PC3e scores increase to the surface of the peat, most
317 probably due to biocycling.

318

319 *Characterization of peat organic matter: FTIR bands, C/N, $\delta^{13}C$, $\delta^{15}N$ and DPH*

320

321 Trends in organic matter properties (C/N, $\delta^{13}\text{C}$, $\delta^{15}\text{N}$ and DPH) and selected FTIR bands are
322 shown in Figure 6. Three principal components (PCo), which explain 86% of the total
323 variance, were extracted from these data (Table SI3). The first principal component (PC1o)
324 accounts for 48% of the total variance. Bands representative of recalcitrant compounds such
325 as aliphatics (2852 cm^{-1} and 2922 cm^{-1}), lignins (1514 cm^{-1}), aromatics (3051 cm^{-1}), amides
326 (1660 cm^{-1} and 1550 cm^{-1}), and $\delta^{15}\text{N}$ – the enrichment of which has been associated with peat
327 decomposition (Létolle, 1980; Macko et al., 1993; Högber, 1997) – show high positive factor
328 loadings. C/N ratio has a high negative loading, while $\delta^{13}\text{C}$ and DPH show moderate negative
329 loadings. Decomposition via residual enrichment of N relative to C (Malmer and Holm,
330 1984; Kuhry and Vitt, 1996) is associated with a decrease in the C/N ratio. The large
331 contribution of recalcitrant compounds, $\delta^{15}\text{N}$ and C/N ratios in this component indicates that
332 the factor is heavily related to the decomposition of peat organic matter. Even variables with
333 moderate loadings support this interpretation, as decreases in $\delta^{13}\text{C}$ in peatlands have been
334 associated with enrichment of recalcitrant moieties (Alewell et al., 2011; Broder et al., 2012;
335 Biester et al., 2013). Recalcitrant plant fractions appear to be more depleted in ^{13}C compared
336 to the bulk plant material; for example, $\delta^{13}\text{C}$ in *Spartina* detritus gradually decreases during
337 biogeochemical processing due to the preservation of substances like lignin which contain
338 less ^{13}C (Benner et al., 1987). Similarly, studies performed on C4 grasses indicate that lignin-
339 C is up to 4.7‰ lower in ^{13}C compared with the bulk plant material (Schweizer et al., 1999).
340 As decomposition leads to an increase in solubilized humic acids, DPH has been widely used
341 as a measure of the degree of peat decomposition (Blackford and Chambers, 1993, 1995;
342 Borgmark, 2005; Borgmark and Schoning, 2006). From 35-15 cm, positive factor scores (Fig.
343 7) indicate a relatively high degree of decomposition compared to the rest of the core,
344 although a generally decreasing pattern of values is detected, reflecting the depth-time
345 dependent nature of decomposition. Lower scores from 29-25 cm and 20-16 cm coincide with

346 smaller amounts of recalcitrant compounds. From 15cm to the surface, scores become
347 negative, indicating a trend to less decomposed/fresh plant remains.
348

349 PC2o accounts for 23% of the total variance. Bands at 1271 cm⁻¹, 1419 cm⁻¹, 1450 cm⁻¹ and
350 1720 cm⁻¹, show high positive loadings. These bands are indicative of lignin, with the
351 exception of that at 1720 cm⁻¹, which represents carboxylic groups. δ¹³C shows a moderate
352 negative loading. The fractionation of commonalities (Table SI3) suggests that lignin and
353 carboxylic acids are related, although with different magnitude, to both PC1o and PC2o. This
354 implies that there are at least two factors affecting lignin and carboxylic groups in the peat.
355 Decomposition (as outlined above) is one of the factors affecting the distribution of lignin,
356 but a more complex behaviour (in addition to that of depth enrichment) is indicated by PC2o.
357 Factor scores (Fig. 7) show an alternating distribution between positive and negative values,
358 except for the section between 20-14 cm, where they are around zero. Factor scores are
359 positive (i.e. the lignin content is higher) at 33-29 cm, 22-21 cm and 8-5 cm.
360

361 The third principal component (PC3o) accounts for 15% of the total variance. Bands of
362 polysaccharides (1070 cm⁻¹ and 1030 cm⁻¹) show high positive loadings (Table SI3) while the
363 band at 3051 cm⁻¹ (aromatics) shows moderate negative loadings. Peat decomposition leads to
364 an enrichment in recalcitrant compounds (e.g. aliphatics and aromatics) of the organic matter
365 as reflected by PC1o. PC3o seems to denote reduced decomposition of labile compounds (i.e.
366 polysaccharides). Changes in vegetation type may also have affected the character of organic
367 matter comprising the peat, and consequently the distribution of polysaccharides. PC3o factor
368 scores indicate heavy enrichment in polysaccharides between 21 and 18 cm (Fig. 7). Smaller
369 increases are found at 35-32 cm, 30.5 cm, 27-25 cm and 12-5 cm.
370

371 **Discussion**

372

373 *Mineral content of the peat: a link with induced soil erosion*

374

375 Although it is possible that some of the lithogenic component might be sourced over long
376 distances, our results suggest that local dusts dominate the signal of major and trace
377 lithogenic elements. The geochemical composition of the peat, and the association of
378 chemical elements in PC1e, is consistent with the character of the local geology (which is
379 composed mostly of granites and gneises). Furthermore, the main chemical ratios (Ti/Zr,
380 K/Rb; Fig. 8), which are commonly applied to determine changes in lithogenic sources, are
381 near-constant through the profile, just increasing after the 1980's, indicating a quite constant
382 composition of the mineral matter until last decades. Increased soil instability linked to
383 human activity may be evidenced at Sandhavn by the enhanced mineral content of the peat
384 and a suite of lithogenic elements (indicated by PC1e; Fig. 8). This would seem to reflect
385 aeolian inputs which are highest (albeit steadily declining in concentration) through a period
386 which is coincident with the end of the Norse settlement at the site. A caveat is required,
387 however, as the peat geochemical record from Sandhavn commences during the settlement
388 phase, which means there are no baseline environmental measurements available prior to the
389 arrival of people. Moreover, this enrichment is registered immediately from above the contact
390 with the mineral (sand) base, where sediment mixing might account for a part of the
391 variation. Pollen and coprophilous fungi evidence intimate that land-use-induced erosion may
392 have still played a role in the enrichment of mineral matter during the earliest stage of peat
393 development. The decline in the mineral content of the peat (PC1e; Figs. 4 and 5) to lower
394 values after ~AD 1400 coincides with reduced frequencies of fungal spores and Poaceae
395 pollen (Figs. 3 and 8). This pattern reflects the Norse abandonment at Sandhavn (Golding et

396 al., 2011), occurring at approximately the same time as many other farms across the Eastern
397 Settlement were also falling into disuse (Edwards et al., 2011; Ledger et al., 2014). A number
398 of other studies from the Eastern Settlement of Greenland have produced convincing
399 evidence for an increase in soil erosion following Norse *landnám* on the basis of rising
400 mineral content in peat or lake sediments (e.g. Sandgren and Fredskild, 1991; Fredskild,
401 1992; Edwards et al., 2008; Massa et al., 2012). At Sandhavn, the concentrations of
402 lithogenic elements remain low throughout the LIA and show little variation until ~AD 1900.
403
404 Massa et al. (2012) noted that Ti remained elevated (14% above pre-*landnám* baseline
405 concentrations) at Lake Igaliku for more than four centuries after the farmstead at *Garðar*
406 (modern Igaliku) was abandoned. They suggest that Norse occupation may have altered the
407 physicochemistry of the catchment soils, or that a change in climate at the onset of the LIA
408 led to enhanced aeolian deposition (and hence Ti influx) to the lake because of increased
409 wind speeds and storminess that were characteristic features of the climate after ~AD 1425
410 (cf. Dugmore et al., 2007). For the period available for examination, this pattern does not
411 seem to be repeated at Sandhavn. The lack of a clear increase in lithogenics during the LIA at
412 Sandhavn suggests that soil disturbance and exposure to wind erosion may have been
413 spatially limited. Changes in vegetation took place immediately after the abandonment of the
414 farm (zone SAN-3; Fig. 3). The increase in Cyperaceae pollen abundance reflects the likely
415 spread of steppe-like vegetation communities (cf. Böcher et al., 1968) across disused home-
416 field areas and the local extension of mire communities in response to cooler and possibly
417 damper conditions. This change in vegetation cover, following the removal of direct human
418 influence from the landscape, may have restricted the availability of erodible material.
419

420 The next simultaneous increase in most lithogenic elements (PC1e; Fig. 8) occurred in the
421 early 20th century (~AD 1900-1940) and is broadly synchronous with the return of sheep
422 farming to southern Greenland (Jacobsen, 1987; Fredskild, 1988).

423 A number of studies have shown the benefits of integrating chemical data with more
424 traditional proxies such as pollen to reconstruct soil erosion and land use changes (e.g. Hölzer
425 and Hölzer, 1998; Lomas-Clarke and Barber, 2004; Martínez Cortizas et al., 2005; Silva-
426 Sánchez et al., 2014). Most of these studies were conducted in areas of relatively intense
427 human activity and show that both proxies – the pollen and the geochemical record –
428 responded to changing land use and were in good agreement with regional archaeological
429 records. The current study also demonstrates the sensitivity of geochemical proxies to
430 environmental change in a more remote landscape. In such circumstances, human activity
431 was on a relatively reduced scale compared with the significant landscape transformations
432 that have taken place in temperate environments (western Europe, for example). In spite of
433 this, the data from Sandhavn not only clearly discriminated between periods of human
434 activity and abandonment, but also recorded human impacts that appear to closely match the
435 known historical record.

436

437 *Peat growth, carbon accumulation, organic matter decomposition and bromine: links with*
438 *climate change*

439

440 Changes in the rate of peat accumulation at Sandhavn (Fig. 9) apparently reflect broad-scale
441 patterns in the prevailing climate (Barlow, 1994; Dahl-Jensen et al., 1998; Box, 2002), with
442 the cooler temperatures of the LIA coinciding with, and seemingly accounting for, the period
443 of extremely slow peat growth witnessed from ~AD 1400-1800, and generally rising
444 temperatures after this leading to the more rapid build-up of peat over the last ~100-150 cal

445 yr. Autocompaction of the peat, whereby deeper layers become compressed relative to the
446 surface, is likely to have acted to reinforce this pattern. Although controls over the rate of
447 peat accumulation seem clear, the factors leading to paludification are less obvious.

448

449 Organic matter began to accumulate in the basin at Sandhavn from ~AD 1240, suggesting an
450 environmental threshold (climatic or otherwise) had been exceeded. On the basis of the
451 synthesis of various climate proxies, Ogilvie and Jónsson (2001) support the notion of it
452 being slightly colder across the North Atlantic region from ~AD 1250-1900 in comparison to
453 the 20th century. A chironomid record from a lake near Igaliku in southern Greenland also
454 suggests a shift towards cooler conditions from ~AD 1280-1460 (Millet et al. 2014), a
455 timeframe encapsulating the 14th century, the period of lowest temperature in central
456 Greenland during the last 700 years (Barlow et al. 1997). Further evidence to suggest that the
457 regional climate was beginning to deteriorate from the mid-13th century onwards can perhaps
458 be seen in the archaeological record from the Eastern Settlement. There appears to have been
459 a shift in Norse subsistence away from farming towards a marine-based diet (Arneborg et al.,
460 1999; Dugmore et al., 2012), although the timing for this is not precise and there are many
461 caveats (Arneborg et al., 2012). There are also indications of abandonment at some Norse
462 farms (Ledger et al., 2014) but an intensification at others (Ledger et al., 2013). Yet all the
463 above should be viewed against the baseline offered by Kaufman et al. (2009), in which a
464 synthesis of terrestrial climate proxies (lakes sediments, glacier ice and tree rings) for
465 latitudes above 60° N demonstrates a long-term cooling trend in the Arctic spanning the last
466 two millennia, albeit punctuated by centennial-scale periods of greater relative warmth (e.g.
467 AD 900-1060) and more severe cold (e.g. AD 1600-1860).

468

469 The very slow rate of peat growth observed at Sandhavn during the mid-second millennium is
470 mirrored at some other sites across the region. For example, radiocarbon dates from the fen
471 near Tasiusaq (Shotyk et al., 2003), approximately 100 km northwest of Sandhavn,
472 demonstrate very rapid accumulation ($\sim 0.3 \text{ cm yr}^{-1}$) for the period after $\sim \text{AD } 1950$ but
473 extremely slow peat growth ($\sim 0.015 \text{ cm yr}^{-1}$) during the preceding $\sim 950 \text{ cal yr}$. At the nearby
474 site of Qinngua, a hiatus spanning $\sim \text{AD } 1400\text{-}1900$ has been recorded in a peat profile
475 (Schofield et al., 2010). This probably represents a period of zero peat growth, although a
476 hiatus resulting from peat cutting should not be discounted. The cutting of peat may have
477 played a part in creating gaps within late Holocene environmental archives drawn from mires
478 across the region (cf. Schofield et al., 2008), although the importance of its role over any
479 climatically-forced slowdown in peat accumulation due to lowered temperatures is difficult to
480 ascertain. It does seem that high-resolution peat archives covering the mid-second
481 millennium AD may be rare in this region, although some exceptions can be found (cf.
482 Ledger et al., 2014).

483

484 Associated with extremely slow peat growth at Sandhavn is an increase in *Hippuris vulgaris*
485 pollen (Figs. 3 and 9), which is probably indicative of shallow open water (pools) at the bog
486 surface, at least seasonally. Flooding during milder seasons due to increased ice/snow melt,
487 combined with low spring-summer evaporation rates from lower temperatures between $\sim \text{AD}$
488 1400 and 1800 , may have increased the habitat suitable for this taxon. Bromine concentrations
489 in the Sandhavn record also seem to be strongly affected by climate as concentrations remain
490 below $150 \mu\text{gg}^{-1}$ until $\sim \text{AD } 1865$, although values do begin to increase gradually after $\sim \text{AD}$
491 1780 (Fig. 9). Research at Qinngua (Schofield et al., 2010) suggested a possible link between
492 variation in the concentrations of halogens and storminess as rising amounts of Br and Cl in
493 the peat appeared to be correlated with increased levels of Na^+ (sea salt sodium) in the GISP2

494 ice core (a hiatus in the peat profile at Qinngua, spanning the period ~AD 1380–1950,
495 hindered attempts to directly compare the two records). No such link was found at Sandhavn.
496 The incorporation of bromine into peat is a biological oxygen-dependent enzymatic processes
497 (Myneni, 2002; Biester et al., 2004; Leri and Myneni, 2012) and it is possible that cooling
498 would have slowed down the biological activity of micro-organisms involved in the process.
499 Flooding of the mire during milder seasons, most favourable for biological activity, could
500 have also limited the incorporation of Br to the peat, a process which in oceanic areas is
501 mostly dependent on oxygen availability rather than atmospheric deposition (Martínez-
502 Cortizas et al., 2007). Organo-bromine compounds can be dehalogenated under reducing
503 conditions (Mohn and Tiedje, 1992; Monserrate and Häggblom, 1997; Bedard and Dort,
504 1998), but at Sandhavn anoxic environmental conditions were seemingly unsuitable for
505 halogenation of organic compounds, and so this appears less likely to explain the patterns in
506 Br as depicted in the data presented here.

507

508 Some of the variations in the proxies analyzed might have also been affected by solar forcing
509 (Fig. 9), a factor that is considered to be a major influence on LIA cooling (Wigley and Kelly,
510 1990; Lean et al., 1995; Mann et al., 1998; van Geel et al., 1999; Bond et al., 2001).

511 Increased PC3o values at ~AD 1480 and ~AD 1645-1740 broadly coincide with the Spörer
512 and Maunder minima. It is necessary to be circumspect about this surmise given the dating
513 and sample resolution constraints, but if correct, this could indicate that enrichment in
514 polyssacharides (i.e. low degradation of labile organic compounds) might be associated with
515 periods of decreased solar activity. The Br record, which shows systematic low
516 concentrations during the whole LIA, has very low values at ~AD 1480 and ~AD 1645-1740,
517 suggesting that cooler conditions during solar minima may also have strongly limited
518 halogenation in the bog. These patterns indicate a possible link between sunspot minima and

519 reduced microbial activity in the Sandhavn bog. Declines in PC1o also might have occurred
520 during solar minima (Fig. 9), indicating that cooling may have limited the decomposition of
521 organic matter during such intervals. Clearly the data coupling proxy records with minima in
522 solar activity during the last millennium at Sandhavn are only tentative, but such associations
523 have been reported from other studies. Mauquoy et al. (2007) identified increases in
524 *Sphagnum tenellum* and *S. cuspidatum* (indicative of cool, moist climatic conditions) in
525 northwestern European bogs that appear linked to LIA solar minima. In their study of Lake
526 Lehmilampi, Finland, Haltia-Hovi et al. (2007) noted a relationship between varve thickness
527 and solar forcing, although the physical mechanism linking these is still to be established.
528 Blackford and Chambers (1995b) also found an apparent correspondence between peat
529 humification records and solar oscillations in Irish blanket peat.

530

531 Beginning ~AD 1870, a major change in vegetation occurred at Sandhavn with *Empetrum*
532 *nigrum* oceanic heath replacing Cyperaceae-dominated steppe communities (Figs.3 and 9).
533 This, plus a more rapid build-up of peat and PCAR over the last ~100-150 cal yr BP,
534 provides evidence of generally rising temperatures following the end of the LIA. At the same
535 time, PC3o variations indicate enrichment of the peat with polysaccharides; this is despite
536 warmer climatic conditions being more conducive to the decay of organic matter (i.e.
537 polysaccharide degradation). The process appears heavily influenced by peat composition,
538 particularly the increased abundance of *Empetrum nigrum* remains which are more resistant
539 to decomposition than the sedge-dominated vegetation that it replaced. The next simultaneous
540 shift in the organic matter indicators (PC1o and Br), peat growth and PCAR, occurred during
541 the last 50 years and seems to reflect the presence of less decomposed peat, typical of the
542 superficial layers of an active mire.

543

544 *Atmospheric deposition of lead: links with anthropogenic emissions and possible sources*

545

546 Murozumi et al. (1969) first demonstrated that a record of lead pollution, dating back to the
547 mid-18th century and coinciding with European Pb production, was recorded in Greenland ice
548 (at Camp Century, Fig.1). Their findings attest to the long-range transport of pollutants to
549 Greenland from sources in industrialized countries. Subsequent research has extended the
550 onset of Pb pollution, as recorded in Greenland ice, to the early historic period. Studies by
551 Hong et al. (1994) and Rosman et al. (1997) show that Greek and Roman lead and silver
552 mining, and smelting, polluted the middle troposphere of the Northern Hemisphere around
553 two millennia ago. In contrast to the investigations on ice cores, studies of lead contamination
554 using minerotrophic peatlands in southern Greenland (Shotyk et al., 2003; Schofield et al.,
555 2010) have up until this point failed to reveal any significant enrichment in Pb, although
556 Shotyk et al. (2003) suggest that a decrease in the $^{206}\text{Pb}/^{207}\text{Pb}$ ratio noted in minerotrophic
557 peat from Tasiusaq relates to lead pollution originating from the USA in the 20th century.

558

559 The lead record from Sandhavn covers a period of around 700 years, extending back from the
560 present to ~AD 1300 (Fig. 10). Lead concentrations remain below $2.5 \mu\text{g g}^{-1}$ throughout most
561 of the sequence and then progressively increase after ~AD 1845. Maximum Pb levels (16.4 -
562 $19.6 \mu\text{g g}^{-1}$) were reached in the 1960s and 1970s, while later decades are characterized by a
563 progressive decrease. Low loadings of Pb on PC1e indicate that Pb does not share a
564 significant common variation with the lithogenic component along the sequence, intimating
565 that in the majority of the record, Pb appears to be solely the result of atmospheric pollution.
566 In order to normalise for any possible contribution of geogenic Pb to the bog at Sandhavn, we
567 have calculated the Pb/Ti ratio (Fig. 10). Notwithstanding some minor differences,
568 particularly between ~AD 1900 and AD 1940 where some of the Pb seems to be linked with

569 increased soil erosion caused by the return of sheep farming to the region in the early 20th
570 century, the pattern for Pb/Ti is almost the same as that of Pb concentrations: values above
571 the baseline occur only after ~AD 1845, and from there they show a progressive increase
572 which is more pronounced after ~AD 1940, peaking at the end of the AD 1970s, after which
573 values steadily decrease. Recent research on atmospheric lead fluxes modelling in southern
574 Greenland has estimated a maximum value for lead fluxes during the 1960s of $2400 \pm 330 \mu\text{g}$
575 $\text{m}^{-2} \text{yr}^{-1}$ (Massa et al., 2015).

576

577 The onset of lead pollution in the Sandhavn monolith occurs later than in records from the
578 Greenland ice core (Murozumi et al., 1969) and lake sediments (Bindler et al., 2001b), where
579 the highest levels of Pb pollution are recorded from ~AD 1750-1800 onwards. The pattern at
580 Sandhavn is thus in closer agreement with the chronology of events from North America (i.e.
581 the onset of the American industrial revolution) rather than that from Europe. Increased Pb
582 deposition just after ~AD 1850 has been found in several North American records including
583 the Great Lakes region (Graney et al., (1995), Maine (Big Heath and Sargent Mountain
584 Pond), and Massachusetts (Plow Shop and Grove ponds), northeast USA (Norton et al., 1997,
585 2004), Hudson Bay (Imitavik and Far Lakes; Outridge et al., 2002), southern Quebec (Lake
586 Tantaré; Gallon et al., (2005) and Point d'Escuminac, Eastern Canada (Kylander et al., 2009).
587 High levels of Pb pollution at Sandhavn during the 20th century are also in good agreement
588 with the Greenland ice core-based reconstructions made by Murozumi et al. (1969), who
589 ascribed Pb pollution to lead smelting (for the period prior to ~AD 1940) and to the massive
590 use of lead alkyls in gasoline (after ~AD 1940). Given that the dating uncertainty of
591 sediment/peat records is often high for the 19th century, caution obviously needs to be
592 exercised, and some comparable lead records also exist in Europe (e.g. Weiss et al, 1999).

593

594 A North American source for the lead is also indirectly supported by the presence of
595 *Ambrosia*-type (ragweed) in the Sandhavn pollen record (Fig. 3). After ~AD 1885, *Ambrosia*-
596 type pollen is consistently present at trace values (typically <1%). *Ambrosia* is a common
597 weed of cultivated land and a prolific pollen producer. The plant is not native to Greenland
598 (Böcher et al., 1968) and, although morphologically-similar pollen is produced by plants
599 present throughout central Europe from the Iron Age forwards, the most likely source for this
600 pollen type is North America. Studies from eastern-central North America (Bassett and
601 Terasmae, 1962; Gordon, 1966; Brugam, 1978; McAndrews, 1988; McAndrews and Boyko-
602 Diakonow, 1989; Baker et al., 1993; Ireland et al. 2014) have demonstrated a rise in
603 *Ambrosia* pollen coinciding with the arrival and expansion of European settlers. It seems that
604 the introduction of intensive agricultural practices linked with forest clearance promoted the
605 increase in *Ambrosia*-type pollen. This pattern has been dated to the 19th century, with only
606 one paper (Brugam, 1978) suggesting an earlier date. The timing of the ‘*Ambrosia* rise’ in
607 North America closely matches the presence of *Ambrosia*-type pollen in the Sandhavn
608 monolith. Bassett and Terasmae (1962) showed that ragweed pollen can be transported
609 through the atmosphere at least 600 km from any known source. Observations of long-
610 distance pollen transport to southern Greenland similarly indicate that northeastern North
611 American source areas are typical (Rousseau, 2003; Rousseau et al., 2006; Jessen et al.
612 2011). A source outside North America seems improbable; for example, *Ambrosia* is a recent
613 introduction to Europe, first appearing after ~AD 1920 (Comtois, 1998) and spreading after
614 the 1980s (Couturier, 1992; Dechamp and Dechamp, 1992; Thibaudon, 1992).

615

616 Cryptotephrae have been recorded in peat profiles located adjacent to Norse sites in the
617 Eastern Settlement and further demonstrate the potential for atmospheric particulates to reach
618 southern Greenland from North America. Blockley et al. (2015) have identified tephra shards

619 at three sites in the Eastern Settlement (Herjolfsnes, Hvalsey and Igaliku). These have
620 geochemical signatures that are compatible with volcanic centres in the Aleutian Islands and
621 Cascade Range, with the Augustine and Mount St Helen volcanoes being two of the likely
622 sources.

623

624 Although a major North American source for the lead at Sandhavn seems most probable and
625 is consistent with results from other studies, some qualifications remain. Rosman et al. (1993,
626 1994) analysed the Pb isotopic composition of Greenland snow collected at Summit to derive
627 the relative lead contributions from the USA, Canada, and Eurasia between ~AD 1967 and
628 1989. They concluded that the United States was a significant source of lead during the 1970s
629 (up to 67% of the measured total) before it declined considerably in relative importance (to
630 25% in the late 1980s), mirroring reductions in the use of leaded petrol, resulting in the
631 Eurasian and Canadian contribution to the Pb signal becoming predominant. Seasonal
632 investigations on the isotopic composition of Pb on snow collected at Dye 3 in southern
633 Greenland also suggest that most of the Pb pollution signal was primarily sourced from
634 leaded gasoline used in North America, but also that the same ice sheet surface received lead
635 from elsewhere during certain parts of the year: Pb in autumn and winter snow originated in
636 North America, while that in spring to mid-summer snow was from Eurasia (Rosman et al.,
637 1998). In contrast, a recent isotopic analysis of west Greenland (near Kangerlussuaq) lake
638 sediments (Bindler et al., 2001a, 2001b) suggests that the lead record at this location was
639 derived from west European and Russian sources. The relative location/latitude of the sites
640 (Fig. 1a) possibly accounts for the differences in lead sourcing. For example, studies have
641 shown that high Arctic sites have largely Russian sources with pollutants transported over the
642 North Pole, whereas lakes in southwest Greenland are considered to have a significant input
643 from west European sources (Bindler et al., 2001b). The lead isotopic signature from aerosol

644 and snowpack samples from Devon Island and from the Canadian High Arctic (Sturges and
645 Barrie, 1989; Shotyk et al., 2005), and from a lake in Pearyland (Lake G07-10), north
646 Greenland, favour a Eurasian source (Michelutti et al., 2009). The origin of lead deposited in
647 Lake CF8 near Nunavut, Baffin Island, could not be determined unequivocally, but
648 investigators suggested an American source to be unlikely (ibid.). In contrast, the evidence
649 from Sandhavn supports atmospheric transfer from North America. Lead isotopic analysis is
650 in progress to ascertain more precisely the sources for lead in the Sandhavn record, and
651 clearly more research is required if a full understanding of the spatial and temporal variation
652 in lead isotopic signatures across Greenland is to be achieved.

653

654 **Conclusions**

655

656 The Norse Age section of the Sandhavn peat profile may be compromised in its basal
657 sand/peat interface segment, but variations in the mineral content of the overlying peat may
658 be partly related to local human activity during the later stages of Norse occupation. A
659 subsequent increase in the lithogenic content during the early 20th century may reflect soil
660 erosion resulting from the return of (modern) sheep farming to southern Greenland.

661

662 Low concentrations of Br are recorded during the LIA – a climatic downturn which is also
663 reflected in extremely low peat accumulation rates at Sandhavn from ~AD 1400-1800. Cold
664 conditions, possibly combined with flooding of the mire surface during milder seasons, which
665 would have created reducing conditions, appear to have caused a slowdown in halogenation
666 that affected Br incorporation into the peat. Low Br concentrations and changes in levels of
667 polysaccharides are possibly in phase with sunspot cycles (Spörer and Maunder minima),
668 though confirmation of a direct link between these parameters and solar activity will require

669 further testing. The local expansion of *Empetrum nigrum* oceanic heath at the end of the 19th
670 century seems to have caused an attendant enrichment in polysaccharides within the peat,
671 suggesting that vegetation type was a major influence over peat organic matter composition
672 at this time.

673

674 The site at Sandhavn has proven more useful for reconstructing a record of lead pollution in
675 southern Greenland than the minerotrophic fen peats that have previously been investigated
676 for this purpose. At Sandhavn, atmospheric Pb pollution is recorded after ~AD 1845, with
677 peak concentrations occurring during the AD 1970s. There is indirect evidence of a
678 predominantly North American origin for this signal. Isotopic analyses will be required
679 before the sources for the lead deposited around the southern tip of Greenland can be
680 identified with greater certainty.

681

682 **Acknowledgements**

683

684 This research was made possible through funding provided by the Leverhulme Trust, the
685 Spanish Ministry of Science and Innovation (Project CGL2010-20672) and Xunta de Galicia
686 (grants R2014/001 and GPC2014/009). N Silva-Sánchez is currently supported by a FPU pre-
687 doctoral grant (AP2010-3264) funded by the Spanish Government. Kirsty Golding, Andy
688 McMullen, and Ian Simpson are thanked for their assistance with fieldwork. Alison Sandison
689 produced the maps. Pete Langdon and two anonymous referees are thanked for comments
690 that helped to improve the paper.

691

692 **References**

- 693 Alewell, C., Giesler, R., Klaminder, J., Leifeld, J., Rollog, M., 2011. Stable carbon isotopes
694 as indicators for environmental change in peat bogs. *Biogeosciences* 8, 1769–1778.
- 695 Allaart, J.H., 1976. Ketilidian mobile belt in south Greenland, in: Escher, A., Stuart-Watt, W.
696 (Eds.), *Geology of Greenland*. Geological Survey of Greenland, Copenhagen, pp. 120–
697 151.
- 698 Appleby, P., 2001. Chronostratigraphic techniques in recent sediments, in: Last, W., Smol, J.
699 (Eds.), *Tracking Environmental Change Using Lake Sediments. Volume 1: Basin*
700 *Analysis, Coring and Chronological Techniques*. Kluwer, Dordrecht, pp. 171–204.
- 701 Appleby, P., Nolan, P., Oldfield, F., Richardson, N., Higgitt, S., 1988. ²¹⁰Pb dating of lake
702 sediments and ombrotrophic peats by gamma assay. *Science of the Total Environment*
703 69, 157–177.
- 704 Appleby, P., Oldfield, F., 1978. The calculation of Pb-210 dates assuming a constant rate of
705 supply of unsupported Pb-210 to the sediment. *Catena* 5, 1–8.
- 706 Arneborg, J., 2006. Saga trails – Brattahlíð, Garðar, Hvalsey Fjord’s Church and Herjolfsnes:
707 four chieftain’s farmsteads in the Norse settlement of Greenland. A visitor’s guidebook.
708 National Museum of Denmark, Nanortalik Museum, Narsaq Museum and Qaqortoq
709 Museum.
- 710 Arneborg, J., Heinemeier, N., Lynnerup, N., Nielsen, H.L., Rud, N., Sveinbjornsdottir, A.E.,
711 1999. Change of diet of the Greenland Vikings determined from stable carbon isotope
712 analysis and C-14 dating of their bones. *Radiocarbon* 14, 157–168.
- 713 Arneborg, J., Lynnerup, N., Heinemeier, J. 2012. Human diet and subsistence patterns in
714 Norse Greenland AD c. 980-AD c.1450: Archaeological interpretations. *Journal of the*
715 *North Atlantic, Special Volume 3*, 119-133.
- 716 Baker, R.G., Schwert, D.P., Bettis, E.A., Chumbley, C.A., 1993. Impact of Euro-American
717 settlement on a riparian landscape in northeast Iowa, midwestern USA: an integrated
718 approach based on historical evidence, floodplain sediments, fossil pollen, plant
719 macrofossils and insects. *The Holocene* 3, 314–323.
- 720 Barlow, L.K., 1994. Evaluation of seasonal to decadal scale deuterium and deuterium excess
721 signals, GISP2 ice core, Summit, Greenland, A.D. 1270-1985. PhD thesis. University of
722 Colorado.
- 723 Bassett, I.J., Terasmae, J., 1962. Radweeds, *Ambrosia* species, in Canada and their history in
724 postglacial time. *Canadian Journal of Botany* 40, 141–150.
- 725 Bedard, D.L., Dort, H.M. Van, 1998. Complete reductive dehalogenation of brominated
726 biphenyls by anaerobic microorganisms in sediment. *Applied and Environmental*
727 *Microbiology* 64, 940–947.

- 728 Benner, R., Fogel, M.L., Sprague, E.K., Hodson, R.E., 1987. Depletion of ¹³C in lignin and
729 its implications for stable carbon isotope studies. *Nature* 329, 708–710.
- 730 Biester, H., Keppler, F., Putschew, A., Martinez-Cortizas, A., Petri, M., 2004. Halogen
731 retention, organohalogens, and the role of organic matter decomposition on halogen
732 enrichment in two Chilean peat bogs. *Environmental Science & Technology* 38, 1984–
733 1991.
- 734 Biester, H., Knorr, K.-H., Schellekens, J., Basler, A., Hermanns, Y.-M., 2013. Comparison of
735 different methods to determine the degree of peat decomposition in peat bogs.
736 *Biogeosciences Discussions* 10, 17351–17395.
- 737 Bindler, R., Anderson, N.J., Renberg, I., Malmquist, C., 2001a. Palaeolimnological
738 investigation of atmospheric pollution in the Søndre Strømfjord region, southern West
739 Greenland: accumulation rates and spatial patterns. *Geology of Greenland Survey*
740 *Bulletin* 53, 48–53.
- 741 Bindler, R., Renberg, I., John Anderson, N., Appleby, P.G., Emteryd, O., Boyle, J., 2001b.
742 Pb isotope ratios of lake sediments in West Greenland: inferences on pollution sources.
743 *Atmospheric Environment* 35, 4675–4685.
- 744 Blaauw, M., 2010. Methods and code for “classical” age-modelling of radiocarbon
745 sequences. *Quaternary Geochronology* 5, 512–518.
- 746 Blackford, J., Chambers, F., 1993. Determining the degree of peat decomposition for peat-
747 based palaeoclimatic studies. *International Peat Journal* 5, 7–24.
- 748 Blackford, J.J., Chambers, F.M., 1995. Proxy climate record for the last 1000 years from Irish
749 blanket peat and a possible link to solar variability. *Earth and Planetary Science Letters*
750 133, 145–150.
- 751 Blockley, S.P.E., Edwards, K.J., Schofield, J.E., Pyne-O’Donnell, S.D.F., Matthews, I.P.,
752 Jensen, B.J.L., Cook, G.T., 2015. First evidence of cryptotephra in palaeoenvironmental
753 records associated with Norse occupation sites in Greenland. *Quaternary Geochronology*
754 27, 145–157.
- 755 Böcher, T.W., Holmer, K., Jakobsen, K., 1968. The flora of Greenland. Haase & Son,
756 Copenhagen.
- 757 Bond, G., Kromer, B., Beer, J., Muscheler, R., Evans, M.N., Showers, W., Hoffmann, S.,
758 Lotti-Bond, R., Hajdas, I., Bonani, G., 2001. Persistent solar influence on North Atlantic
759 climate during the Holocene. *Science* 294, 2130–6.
- 760 Borgmark, A., 2005. Holocene climate variability and periodicities in south-central Sweden,
761 as interpreted from peat humification analysis. *The Holocene* 15, 387–395.
- 762 Borgmark, A., Schoning, K., 2006. A comparative study of peat proxies from two eastern
763 central Swedish bogs and their relation to meteorological data. *Journal of Quaternary*
764 *Science* 21, 109–114.

- 765 Box, J., 2002. Study of Greenland instrument temperature records: 1873-2001. *International*
766 *Journal of Climatology* 22, 1829–1847.
- 767 Broder, T., Blodau, C., Biester, H., Knorr, K.H., 2012. Peat decomposition records in three
768 pristine ombrotrophic bogs in southern Patagonia. *Biogeosciences* 9, 1479–1491.
- 769 Brugam, R.B., 1978. Pollen indicators of land-use change in southern Connecticut.
770 *Quaternary Research* 9, 349–362.
- 771 Chambers, F.M., Booth, R.K., De Vleeschouwer, F., Lamentowicz, M., Le Roux, G.,
772 Mauquoy, D., Nichols, J.E., van Geel, B., 2012. Development and refinement of proxy-
773 climate indicators from peats. *Quaternary International* 268, 21–33.
- 774 Cheburkin, A.K., Shotyk, W., 1996. An energy dispersive miniprobe multielement analyzer
775 (EMMA) for direct analysis of Pb and other trace elements in peat. *Journal of Analytical*
776 *Chemistry* 354, 688–691.
- 777 Chesworth, W., Martínez Cortizas, A., García-Rodeja, E., 2006. The redox-pH approach to
778 the geochemistry of the Earth's land surface, with application to peatlands, in: Martini,
779 I.P., Martínez Cortizas, A., Chesworth, W. (Eds.), *Peatlands: Evolution and Records of*
780 *Environmental and Climate Changes*. Amsterdam, pp. 175–196.
- 781 Cocozza, C., D'Orazio, V., Miano, T.M., Shotyk, W., 2003. Characterization of solid and
782 aqueous phases of a peat bog profile using molecular fluorescence spectroscopy, ESR
783 and FT-IR, and comparison with physical properties. *Organic Geochemistry* 34, 49–60.
- 784 Comtois, P., 1998. Ragweed (*Ambrosia* sp.): the phoenix of allergophytes, in: Spieksma,
785 F.T.M. (Ed.), *Ragweed in Europe*. 6th Int. Congr. Aerobiol. Satellite Symp. Proc.
786 Horsholm DK, Perugia, pp. 3–5.
- 787 Couturier, P., 1992. Dispersion of ragweed in the Drome-Ardeche region. *Allergie et*
788 *immunologie* 24, 27–31.
- 789 Dahl-Jensen, D., Mosegaard, K., Gundestrup, N., Clow, G.G.D., Johnsen, S.S.J., Hansen,
790 A.A.W., Balling, N., Clow, D.G., 1998. Past temperatures directly from the Greenland
791 ice sheet. *Science* 282, 268–271.
- 792 Dechamp, C., Dechamp, J., 1992. Ragweed pollen counts (P. Cour collection apparatus) from
793 Lyon-Bron from 1982 to 1989: results, informing the public. *Allergie et immunologie*
794 24, 17 – 21.
- 795 Dugmore, A.J., Borthwick, D.M., Church, M.J., Dawson, A., Edwards, K.J., Keller, C.,
796 Mayewski, P., McGovern, T.H., Mairs, K-A. Sveinbjarnardóttir, G., 2007. The role of
797 climate in settlement and landscape change in the North Atlantic islands: an assessment
798 of cumulative deviations in high-resolution proxy records. *Human Ecology* 35, 169–178.
- 799 Dugmore, A.J., Church, M.J., Buckland, P.C., Edwards, K.J., Lawson, I., McGovern, T.H.,
800 Panagiotakopulu, E., Simpson, I. a., Skidmore, P., Sveinbjarnardóttir, G., 2005. The
801 Norse landnám on the North Atlantic islands: an environmental impact assessment.
802 *Polar Record* 41, 21–37.

- 803 Dugmore, A.J., McGovern, T.H., Vésteinsson, O., Arneborg, J., Streeter, R., Keller, C. 2012.
804 Cultural adaptation, compounding vulnerabilities and conjunctures in Norse Greenland.
805 Proceedings of the National Academy of Sciences 109, 3658-3663.
- 806 Edwards, K.J., Schofield, J.E., Kirby, J.R., Cook, G.T., 2011. Problematic but promising
807 ponds? Palaeoenvironmental evidence from the Norse Eastern Settlement of Greenland.
808 Journal of Quaternary Science 26, 854-865.
- 809 Edwards, K.J., Schofield, J.E., Mauquoy, D., 2008. High resolution paleoenvironmental and
810 chronological investigations of Norse landnám at Tasiusaq, Eastern Settlement,
811 Greenland. Quaternary Research 69, 1–15.
- 812 Eriksson, L., Johansson, E., Kettaneh-Wold, N., Wold, S., 1999. Introduction to multi- and
813 megavariate data analysis using projection methods (PCA & PLS). Umetrics AB, Umea.
- 814 Feilberg, J., 1984. A phytogeographical study of south Greenland. Bioscience 15, 1–70.
- 815 Fitzhugh, W.W., Ward, E.I., 2000. Vikings: the North Atlantic saga. Smithsonian Institution
816 Press, Washington.
- 817 Fredskild, B., 1988. Agriculture in a Marginal area- South Greenland from the Norse
818 Landnam (985 A.D.) to the present (1985 A.D.), in: Birks, H.H., Birks, H.J.B., Kaland,
819 P.E., Moe, D. (Eds.), The Cultural Landscape—Past, Present and Future. Cambridge
820 University Press, Cambridge, pp. 381–393.
- 821 Fredskild, B., 1992. Erosion and vegetational changes in South Greenland caused by
822 agriculture. Geografisk Tidsskrift 92, 14–21.
- 823 Gallon, C., Tessier, A., Gobeil, C., Beaudin, L., 2005. Sources and chronology of
824 atmospheric lead deposition to a Canadian Shield lake: inferences from Pb isotopes and
825 PAH profiles. Geochimica et Cosmochimica Acta 69, 3199–3210.
- 826 Golding, K.A., Simpson, I.A., Schofield, J.E., Edwards, K.J., 2011. Norse-Inuit interaction
827 and landscape change in southern Greenland? A geochronological, Pedological, and
828 Palynological investigation. Geoarchaeology: an international journal 26, 315–345.
- 829 Golding, K.A., Simpson, I.A., Wilson, C.A., Lowe, E.C., Schofield, J.E., Edwards, K.J.,
830 2014. Europeanization of sub-Arctic environments: perspectives from Norse Greenland's
831 outer fjords. Human Ecology.
- 832 González, J.A., González-Vila, F.J., Almendros, G., Zancada, M.C.C., Polvillo, O., Martín,
833 F., 2003. Preferential accumulation of selectively preserved biomacromolecules in the
834 humus fractions from a peat deposit as seen by analytical pyrolysis and spectroscopic
835 techniques. Journal of Analytical and Applied Pyrolysis 68-69, 287–298.
- 836 Gordon, J.G., 1966. Forest History of Ohio . I , Radiocarbon Dates and Pollen Stratigraphy of
837 Silver Lake , Logan County , Ohio. The Ohio Journal of Science 66, 387–400.

- 838 Graney, J., Halliday, A., Keeler, G., Nriagu, J., Robbins, J., Norton, S., 1995. Isotopic record
839 of lead pollution in lake sediments from the northeastern United States. *Geochimica et*
840 *Cosmochimica Acta* 59, 1715–1728.
- 841 Grimm, E.C., 1992. Tilia. Version 2.0.
- 842 Grimm, E.C., 2004. TGView.
- 843 Grove, J., 1988. *The Little Ice Age*. Methuen, London.
- 844 Grube, M., Lin, J.G., Lee, P.H., Kokorevicha, S., 2006. Evaluation of sewage sludge-based
845 compost by FT-IR spectroscopy. *Geoderma* 130, 324–333.
- 846 Guo, Y., Bustin, R.M., 1998. FTIR spectroscopy and reflectance of modern charcoals and
847 fungal decayed woods: implications for studies of inertinite in coals. *International*
848 *Journal of Coal Geology* 37, 29–53.
- 849 Haberhauer, G., Rafferty, B., Strebl, F., Gerzabek, M.H., 1998. Comparison of the
850 composition of forest soil litter derived from three different sites at various
851 decompositional stages using FTIR spectroscopy. *Geoderma* 83, 331–342.
- 852 Haltia-Hovi, E., Saarinen, T., Kukkonen, M., 2007. A 2000-year record of solar forcing on
853 varved lake sediment in eastern Finland. *Quaternary Science Reviews* 26, 678–689.
- 854 Högber, P., 1997. ^{15}N natural abundance in soil-plant systems. *New Phytologist* 137, 179–
855 203.
- 856 Hölzer, A., 1998. Silicon and titanium in peat profiles as indicators of human impact. *The*
857 *Holocene* 8, 685–696.
- 858 Hong, S., Candelone, J.J.-P., Patterson, C.C., Boutron, C.F., Civilizations, R., 1994.
859 Greenland Ice Evidence of Hemispheric Lead Pollution Two Millennia Ago by Greek
860 and Roman Civilizations. *Science* 265, 1841–1843.
- 861 Ibarra, J. V, Muñoz, E., Moliner, R., 1996. FTIR study of the evolution of coal structure
862 during the coalification process. *Organic Geochemistry* 24, 725–735.
- 863 Ireland, A.W., Clifford, M.J., Booth, R.K., 2014. Widespread dust deposition on North
864 American peatlands coincident with European land-clearance. *Vegetation History &*
865 *Archaeobotany* 23, 693-700.
- 866 Jacobsen, N.K., 1987. Studies on soils and potential for soil erosion in the sheep farming area
867 of South Greenland. *Arctic and Alpine Research* 19, 498–507.
- 868 Jessen, C.A., Solignac, S., Nørgaard-Pedersen, N., Mikkelsen, N., Kuijpers, A., Siedenkrantz,
869 M.-S., 2011. Exotic pollen as an indicator of variable atmospheric circulation over the
870 Labrador Sea region during the mid to late Holocene. *Journal of Quaternary Science* 26,
871 286-296.

- 872 Kaufman, D.S., Schneider, D.P., McKay, N.P., Ammann, C.M., Bradley, R.S., Briffa, K.R.,
873 Miller, G.H., Otto-Bliesner, B.L., Overpeck, J.T., Vinther, B.M., Arctic Lakes 2k project
874 members, 2009. Recent warming reverses long-term Arctic cooling. *Science* 325, 1236–
875 1239. doi:10.1126/science.1173983
- 876 Krogh, K.J., 1967. *Viking Greenland*. National Museum, Copenhagen.
- 877 Kuhry, P., Vitt, D.H., 1996. Fossil carbon/nitrogen ratios as a measure of peat decomposition.
878 *Ecology* 77, 271–275.
- 879 Kylander, M.E., Weiss, D.J., Kober, B., 2009. Two high resolution terrestrial records of
880 atmospheric Pb deposition from New Brunswick, Canada, and Loch Laxford, Scotland.
881 *The Science of the Total Environment* 407, 1644–57.
- 882 Lean, J., Beer, J., Bradley, R., 1995. Reconstruction of solar irradiance since 1610:
883 Implications for climate change. *Geophysical Research Letters* 22, 3195–3198.
- 884 Ledger, P.M., Edwards, K.J., Schofield, J.E., 2013. Shieling activity in the Norse Eastern
885 Settlement: palaeoenvironment of the 'Mountain Farm', Vatnahverfi, Greenland. *The*
886 *Holocene* 23, 810-822.
- 887 Ledger, P.M., Edwards, K.J., Schofield, J.E., 2014. Vatnahverfi: a green and pleasant land?
888 Palaeoecological reconstructions of environmental and land-use change. *Journal of the*
889 *North Atlantic*, Special Volume 6, 29-46.
- 890 Leri, A.C., Myneni, S.C.B., 2012. Natural organobromine in terrestrial ecosystems.
891 *Geochimica et Cosmochimica Acta* 77, 1–10.
- 892 Létolle, R., 1980. Nitrogen-15 in the natural environment, in: Fritz, P., Fontes, J.C. (Eds.),
893 *Handbook of Environmental Isotope Geochemistry*, Vol. 1. Elsevier, Amsterdam, pp.
894 407– 429.
- 895 Lomas-Clarke, S.H.S.H., Barber, K.E.K.E., 2004. Palaeoecology of human impact during the
896 historic period: palynology and geochemistry of a peat deposit at Abbeyknockmoy, Co.
897 Galway, Ireland. *The Holocene* 14, 721–731.
- 898 Macko, S., Entzeroth, L., Parker, P., 1993. Early diagenesis of organic matter in sediments.
899 Assessment of mechanisms and preservation by the use of isotopic molecular
900 approaches, in: Engel, J. (Ed.), *Organic Geochemistry: Principles and Applications*.
901 Plenum, New York, pp. 211–224.
- 902 Malmer, N., Holm, E., 1984. Variation in the C/N-quotient of peat in relation to
903 decomposition rate and age determination with 210 pb. *Oikos* 43, 171–182.
- 904 Mann, M.E., Bradley, R.S., Hughes, M.K., 1998. Global-scale temperature patterns and
905 climate forcing over the past six centuries. *Nature* 392, 779–787.
- 906 Martínez Cortizas, A., López-Merino, L., Bindler, R., Mighall, T., Kylander, M., 2013.
907 Atmospheric Pb pollution in N Iberia during the late Iron Age/Roman times

- 908 reconstructed using the high-resolution record of La Molina mire (Asturias, Spain).
909 *Journal of Paleolimnology* 50, 71–86.
- 910 Martínez Cortizas, A., Mighall, T., Pontevedra Pombal, X., Nóvoa Muñoz, J.C.C., Peiteado
911 Varela, E., Piñeiro Rebolo, R., 2005. Linking changes in atmospheric dust deposition,
912 vegetation change and human activities in northwest Spain during the last 5300 years.
913 *The Holocene* 15, 698–706.
- 914 Martínez-Cortizas, A., Biester, H., Mighall, T., Bindler, R., Mart, A., 2007. Climate-driven
915 enrichment of pollutants in peatlands. *Biogeosciences* 4, 905–911.
- 916 Massa, C., Bichet, V., Gauthier, É., Perren, B.B., Mathieu, O., Petit, C., Monna, F.,
917 Giraudeau, J., Losno, R., Richard, H., 2012. A 2500 year record of natural and
918 anthropogenic soil erosion in South Greenland. *Quaternary Science Reviews* 32, 119–
919 130.
- 920 Massa, C., Monna, F., Bichet, V., Gauthier, E., Losno, R., Richard, H. 2015. Inverse
921 modeling of past lead atmospheric deposition in South Greenland. *Atmospheric*
922 *Environment* 105, 121-129.
- 923 Matthews, J.A., Briffa, K.R., 2005. The “Little Ice Age”: re-evaluation of an evolving
924 concept. *Geografiska Annaler* 87, 17–36.
- 925 Mauquoy, D., Geel, B. Van, Blaauw, M., Plicht, J. Van Der, 2007. Evidence from northwest
926 European bogs shows “ Little Ice Age ” climatic changes driven by variations in solar
927 activity. *The Holocene* 1, 1–6.
- 928 McAndrews, J.H., 1988. Human disturbance of North American forests and grasslands: the
929 fossil pollen record, in: Huntley, B., Webb, T. (Eds.), *Vegetation History Volume of*
930 *Handbook of Vegetation Science Series*. Kluwer Academic Publishers, Utrech, pp. 673–
931 697.
- 932 McAndrews, J.H., Boyko-Diakonow, M., 1989. Pollen analysis of varved sediment at
933 Crawford lake, Ontario: evidence of Indian and European farming, in: Fulton, R.D. (Ed.),
934 *Quaternary Geology of Canada and Greenland*. Geological Survey of Canada, Ottawa,
935 pp. 528–530.
- 936 Meharg, A.A.A., Edwards, K.J.J., Schofield, J.E.E., Raab, A., Feldmann, J., Moran, A.C.,
937 Bryant, C.L.L., Thornton, B., Dawson, J. J.C., 2012. First comprehensive peat
938 depositional records for tin, lead and copper associated with the antiquity of Europe’s
939 largest cassiterite deposit. *Journal of Archaeological Science* 39, 717–727.
- 940 Michelutti, N., Simonetti, A., Briner, J.P., Funder, S., Creaser, R. a, Wolfe, A.P., 2009.
941 Temporal trends of pollution Pb and other metals in east-central Baffin Island inferred
942 from lake sediment geochemistry. *The Science of the Total Environment* 407, 5653–
943 5662.
- 944 Millet, L., Massa, C., Bichet, V., Frossard, V., Belle, S., Gauthier, E., 2014. Anthropogenic
945 versus climatic control in a high-resolution 1500-year chironomid stratigraphy from a
946 southwestern Greenland lake. *Quaternary Research* 81, 193-202.

- 947 Mohn, W., Tiedje, J., 1992. Microbial reductive dehalogenation. *Microbiological and*
948 *Molecular Biology Reviews* 56, 482–507.
- 949 Monserrate, E., Häggblom, M., 1997. Dehalogenation and biodegradation of brominated
950 phenols and benzoic acids under iron-reducing, sulfidogenic, and methanogenic
951 conditions. *Applied and Environmental Microbiology* 63, 3911–3915.
- 952 Moore, G.W.K., Pickart, R.S., Renfrew, I.A., 2008. Buoy observations from the windiest
953 location in the world ocean, Cape Farewell, Greenland. *Geophysical Research Letters*
954 35.
- 955 Moore, P.D., Webb, J.A., Collinson, M.E., 1991. *Pollen Analysis*. 2nd Edition, 2nd editio. ed.
956 Blackwell Scientific Publications, London.
- 957 Murozumi, M., Chow, T.J., Patterson, C., 1969. Chemical concentrations of pollutant lead
958 aerosols, terrestrial dusts and sea salts in Greenland and Antarctic snow strata.
959 *Geochimica et Cosmochimica Acta* 33, 1247–1294.
- 960 Myneni, S.C.B., 2002. Formation of stable chlorinated hydrocarbons in weathering plant
961 material. *Science (New York, N.Y.)* 295, 1039–41.
- 962 Niemeyer, J., Chen, Y., Bollag, J.-M., 1992. Characterization of humic acids, composts, and
963 peat by diffuse reflectance fourier- transform infrared-spectroscopy. *Soil Science*
964 *Society of America Journal* 56, 135–140.
- 965 Norton, S., Evans, G.C., Kahl, J.S., 1997. Comparison of Hg and Pb fluxes to hummocks
966 and hollows of ombrotrophic Big Heath and to nearby Sargent Mt. Pond, Maine. *Water,*
967 *Air, and Soil Pollution* 100, 271–286.
- 968 Norton, S.A., Perry, E.R., Haines, Terry, A., Dieffenbacher-Krallc, A.C., 2004.
969 Paleolimnological assessment of Grove and Plow Shop Ponds, Ayer, Massachusetts,
970 USA – A superfund site. *Journal of Environmental Monitoring* 6, 457–465.
- 971 Ogilvie, A.E.J., Jónsson, T., 2001. "Little Ice Age" research: a perspective from Iceland.
972 *Climatic Change* 48, 9-52.
- 973 Outridge, P.M., Hermanson, M.H., Lockhart, W.L., Utridge, P.M.O., Ermanson, M.H.H.,
974 Ockhart, W.L.L., 2002. Regional variations in atmospheric deposition and sources of
975 anthropogenic lead in lake sediments across the Canadian Arctic. *Geochimica et*
976 *Cosmochimica Acta* 66, 3521–3531.
- 977 Parker, F.S., 1971. *Applications of Infrared Spectroscopy in biochemistry, biology and*
978 *medicine*. Adam Hilger, London.
- 979 Pontevedra-Pombal, X., Mighall, T.M., Nóvoa-Muñoz, J.C., Peiteado-Varela, E., Rodríguez-
980 Racedo, J., García-Rodeja, E., Martínez-Cortizas, A., 2013. Five thousand years of
981 atmospheric Ni, Zn, As, and Cd deposition recorded in bogs from NW Iberia: prehistoric
982 and historic anthropogenic contributions. *Journal of Archaeological Science* 40, 764–
983 777.

- 984 Renfrew, I.A., Petersen, G.N., Outten, S., Sproson, D., Moore, G.W.K., Hay, C., Ohigashi,
985 T., Zhang, S., Kristjánsson, J.E., Førre, I., Ólafsson, H., Gray, S.L., Irvine, E. a., Bovis,
986 K., Brown, P.R. a., Swinbank, R., Haine, T., Lawrence, A., Pickart, R.S., Shapiro, M.,
987 Woolley, A., 2008. The Greenland Flow Distortion Experiment. *Bulletin of the*
988 *American Meteorological Society* 89, 1307–1324.
- 989 Raahauge, K., Hoegh-Knudsen, P., Gulløv, H.C., Mohl, J., Krause, C., Møller, N.A., 2003.
990 Tidlig Thulekultur I Sydgrønland. Rapport om undersøgelserne I Nanortalik Kommune,
991 sommeren 2002, Feltrapport 9. SILA, Nationalmuseets Center for Grønlandsforskning,
992 Copenhagen.
- 993 Rosman, K.J., Chisholm, W., Hong, S., Candelone, J.-P., Boutron, C.F., 1997. Lead from
994 Carthaginian and Roman Spanish Mines Isotopically Identified in Greenland Ice Dated
995 from 600 B.C. to 300 A.D. *Environmental Science & Technology* 31, 3413–3416.
- 996 Rosman, K.J.R., Chisholm, W., Boutron, C.F., Candelone, J.P., Görlach, U., 1993. Isotopic
997 evidence for the source of lead in Greenland snows since the late 1960s. *Nature* 362,
998 333–335.
- 999 Rosman, K.J.R., Chisholm, W., Boutron, C.F., Candelone, J.-P., Jaffrezo, J.-L., Davidson,
1000 C.I., 1998. Seasonal variations in the origin of lead in snow at Dye 3, Greenland. *Earth*
1001 *and Planetary Science Letters* 160, 383–389.
- 1002 Rousseau, D., Schevin, P., Duzer, D., Cambon, G., Ferrier, J., Jolly, D., Poulsen, U., 2006.
1003 New evidence of long distance pollen transport to southern Greenland in late spring.
1004 *Review of Palaeobotany and Palynology* 141, 277–286.
- 1005 Rousseau, D.-D., 2003. Long distance transport of pollen to Greenland. *Geophysical*
1006 *Research Letters* 30, 1765.
- 1007 Sampe, T., Shang-Ping, X., 2007. Mapping high sea winds from space: a global climatology.
1008 *Bulletin of the American Meteorological Society* 88, 1965–1978.
- 1009 Sandgren, P., Fredskild, B., 1991. Magnetic measurements recording Late Holocene man-
1010 induced erosion in S. Greenland. *Boreas* 20, 315–331.
- 1011 Schofield, J.E., Edwards, K.J., 2011. Grazing impacts and woodland management in
1012 Eriksfjord: *Betula*, coprophilous fungi and the Norse settlement of Greenland.
1013 *Vegetation History and Archaeobotany* 20, 181–197.
- 1014 Schofield, J.E., Edwards, K.J., Christensen, C., 2008. Environmental impacts around the time
1015 of Norse landnám in the Qorlortoq valley, Eastern Settlement, Greenland. *Journal of*
1016 *Archaeological Science* 35, 1643–1657.
- 1017 Schofield, J.E., Edwards, K.J., Mighall, T.M., Martínez-Cortizas, A., Rodríguez-Racedo, J.,
1018 Cook, G., Martínez Cortizas, A., 2010. An integrated geochemical and palynological
1019 study of human impacts, soil erosion and storminess from southern Greenland since c.
1020 AD 1000. *Palaeogeography, Palaeoclimatology, Palaeoecology* 295, 19–30.

- 1021 Schweizer, M., Fear, J., Cadisch, G., 1999. Isotopic (^{13}C) fractionation during plant residue
1022 decomposition and its implications for soil organic matter studies. *Rapid*
1023 *communications in mass spectrometry* 13, 1284–1290.
- 1024 Shotyk, W., Goodsite, M.E.E., Roos-Barraclough, F., Frei, R., Heinemeier, J., Asmund, G.,
1025 Lohse, C., Hansen, T.S.S., 2003. Anthropogenic contributions to atmospheric Hg, Pb
1026 and As accumulation recorded by peat cores from southern Greenland and Denmark
1027 dated using the ^{14}C “bomb pulse curve”. *Geochimica et Cosmochimica Acta* 67, 3991–
1028 4011.
- 1029 Shotyk, W., Zheng, J., Krachler, M., Zdanowicz, C., Koerner, R., Fisher, D., 2005.
1030 Predominance of industrial Pb in recent snow (1994–2004) and ice (1842–1996) from
1031 Devon Island, Arctic Canada. *Geophysical Research Letters* 32, L21814.
- 1032 Silva-Sánchez, N., Martínez Cortizas, A., López-Merino, L., 2014. Linking forest cover, soil
1033 erosion and mire hydrology to late-Holocene human activity and climate in NW Spain.
1034 *The Holocene* 24, 714–725.
- 1035 Smidt, E., Meissl, K., Schwanninger, M., Lechner, P., 2008. Classification of waste materials
1036 using Fourier transform infrared spectroscopy and soft independent modeling of class
1037 analogy. *Waste management* 28, 1699–1710.
- 1038 Solomon, D., Lehmann, J., Thies, J., Schafer, T., Liang, B., Kinyangi, J., Neves, E.,
1039 Petersen, J., Luizao, F., Skjemstad, J., 2007. Molecular signature and sources of
1040 biochemical recalcitrance of organic C in Amazonian Dark Earths. *Geochimica*
1041 *Cosmochimica Acta* 71, 2285–2298.
- 1042 Sturges, W.T., Barrie, L.A., 1989. Stable lead isotope ratios in Arctic aerosols: Evidence for
1043 the origin of Arctic air pollution. *Atmospheric Environment* 23, 2513 – 2520.
- 1044 Thibaudon, M., 1992. Ragweed in France; some air pollen data for the years 1987 – 1990.
1045 *Allergie et immunologie* 24, 9– 16.
- 1046 Van Geel, B., Buurman, J., Brinkkemper, O., Schelvis, J., Aptroot, A., van Reenen, G.,
1047 Hakbijl, T., 2003. Environmental reconstruction of a Roman Period settlement site in
1048 Uitgeest (The Netherlands), with special reference to coprophilous fungi. *Journal of*
1049 *Archaeological Science* 30, 873–883.
- 1050 Van Geel, B., Raspopov, O.M., Renssen, H., van der Plicht, J., Dergachev, V. a., Meijer, H.
1051 a. J., 1999. The role of solar forcing upon climate change. *Quaternary Science Reviews*
1052 18, 331–338.
- 1053 Wallbrink, P.J., Walling, D.E., He, Q., 2002. Radionuclide measurement using Hpge Gamma
1054 Spectrometry, in: Zapata, F. (Ed.), *Handbook for the Assessment of Soil Erosion and*
1055 *Sedimentation Using Environmental Radionuclides*. Kluwer, Dordrecht, pp. 67–96.
- 1056 Walling, D.E., He, Q., P.G., A., 2002. Conversion models for soil-erosion, soil-redistribution
1057 and sedimentation investigations, in: Zapata, F. (Ed.), *Handbook for the Assessment of*
1058 *Soil Erosion and Sedimentation Using Environmental Radionuclides*. Kluwer,
1059 Dordrecht, pp. 111–164.

- 1060 Wigley, T., Kelly, P., 1990. Holocene climatic change, 14C wiggles and variations in solar
1061 irradiance. Philosophical Transactions of the Royal Society 330, 547–560.
- 1062 WRB, I.W.G., 2014. World Reference Base for Soil Resources 2014. International soil
1063 classification system for naming soils and creating legends for soil maps. World Soil
1064 Resources Reports No. 106. FAO, Rome.
- 1065 Zaccheo, P., Cabassi, G., Ricca, G., Crippa, L., 2002. Decomposition of organic residues in
1066 soil: experimental technique and spectroscopic approach. Organic Geochemistry 33,
1067 327–345.
- 1068
- 1069

1070 **List of figures**

1071

1072 Figure 1: (a) Map of Greenland and northeast North America showing the locations of sites
1073 and places mentioned in the text. Key to numbering: (1) Plow Shop and Grove Ponds; (2) Big
1074 Heath and Sargent Mountain Pond; (3) Lake Tantaré; (4) Point d'Escuminac; (5) Imitavik
1075 Lake; (6) Far Lake; (7) Lake CF8; (8) Devon Island; (9) Camp Century; (10) Lake G07-01;
1076 (11) Summit; (12) Kangerlussuaq; (13) Sandhavn and Cape Farewell; (b) the area around
1077 Sandhavn, southern Greenland, showing sites and places mentioned in the text; (c) the
1078 sampling location at Sandhavn. The white star marks the position from which the peat
1079 monolith was taken; (d) the landscape around the sampling location at Sandhavn showing the
1080 position of the Norse ruins and former homefields. (Photographs by J.E.Schofield, August
1081 2008).

1082

1083 Figure 2. Age-depth model for Sandhavn (after Golding et al. [2011] with minor changes).
1084 Shaded (greyscale) boxes represent the 2σ calibrated ranges of radiocarbon dates used in the
1085 model; clear boxes are the ^{210}Pb dates (with associated errors). One ^{14}C date – depicted here
1086 in black – was considered to be an outlier and has been removed from the model. The solid
1087 black line connecting the ^{14}C and ^{210}Pb dates represents the 'best estimate' based on the
1088 model, with the grey envelope around this demonstrating the maximum and minimum (95%)
1089 confidence limits.

1090

1091 Figure 3. Percentage pollen diagram for Sandhavn displaying selected taxa (after Golding et
1092 al. [2011] with minor changes). The SAN-2/3 pollen zone boundary represents the
1093 replacement of hayfields and pastures (Poaceae-dominated assemblages) with tundra or
1094 steppe vegetation (Cyperaceae-dominated assemblages), and with it the Norse abandonment

1095 of the site. This vegetation was to persist until around AD 1850 and the development of
1096 *Empetrum nigrum* oceanic heath. *Ambrosia* pollen is recorded in SAN-5. This genus is not
1097 native to southern Greenland (Böcher et al., 1968) and must be part of the long-distance
1098 component arriving at the site. Curves for *Hippuris vulgaris*, *Sporormiella*-type
1099 (coprophilous fungi) and C:P (ratio of charcoal to pollen concentration) act as proxies for the
1100 presence of standing water, grazing by animals, and fires/burning respectively.

1101

1102 Figure 4: LOI and elemental composition through the peat section of the Sandhavn monolith.
1103 Note that x-axes scales and units vary between graphs.

1104

1105 Figure 5: Factor scores for the first three principal components (PC1e, PC2e, and PC3e)
1106 extracted from the PCA performed on LOI and elemental composition data from the peat
1107 section of the Sandhavn monolith. Boxes with dashed outlines indicate sections with higher
1108 PC1e scores (i.e. higher mineral content).

1109

1110 Figure 6. Variations in organic matter indicators through the peat section of the Sandhavn
1111 monolith: (A) C/N ratio, degree of peat humification (DPH), and variations in $\delta^{13}\text{C}$ and $\delta^{15}\text{N}$;
1112 (B) Selected FTIR bands (expressed as z-scores).

1113

1114 Figure 7: Factor scores for the first three principal components (PC1o, PC2o, and PC3o)
1115 extracted from the PCA performed on selected FTIR bands, C/N, $\delta^{13}\text{C}$, $\delta^{15}\text{N}$ and DPH
1116 through the peat section of the Sandhavn monolith.

1117

1118 Figure 8: PC1e factor scores (reflecting the mineral content of the peat), Ti/Zr and K/Rb
1119 plotted against selected pollen types and spores from the Sandhavn monolith.

1120

1121 Figure 9: Selected variables through the Sandhavn monolith. From top to bottom: peat growth
1122 rate and peat carbon accumulation rate (PCAR: grey line) with y-axis truncated such that very
1123 high values recorded after AD 1950 (shown on the embedded graph) are not depicted;
1124 percentage of *Hippuris vulgaris* pollen; Br concentration; levels of recalcitrant compounds in
1125 the peat (reflected by PC1o factor scores); levels of polysaccharides in the peat (reflected by
1126 PC3o factor scores); percentage of *Empetrum nigrum* pollen; variations in $R\delta^{14}C$ (Reimer et
1127 al., 2004). Light grey shading indicates the approximate timeframe of Little Ice Age climate
1128 and dark grey bands indicate the Spörer and Maunder minima in solar activity.

1129

1130 Figure 10: Pb concentration and Pb/Ti ratio (expressed as z-scores) through the peat unit of
1131 the Sandhavn monolith.

1132

1133 Figure SI.1. LOI and elemental composition through the full depth of the monolith (40-0 cm)
1134 from Sandhavn. Note the major changes between the sand layer at the base and the peat
1135 above this.

1136

1137

1138 **List of tables**

1139

1140 Table 1. Radiocarbon dates from Sandhavn. All measurements are AMS on bryophytes
1141 (*Dicranium*, *Drepanocladus*, *Hypnum*, *Hylocomium* and *Racomitrium* spp.). Calendar ranges
1142 are those used by the (*Clam*) age-depth model (Fig. 2) following calibration against the
1143 Intcal13 calibration curve (Reimer et al., 2013). See Golding et al. (2011) for a further
1144 discussion of the radiocarbon dates.

1145

1146 Table SI1. Assignment and characterization of FTIR bands included in the principal
1147 components analysis of the peat organic matter properties from Sandhavn (vertical variation
1148 of bands plotted in Fig. 6).

1149

1150 Table SI2. Factor loadings from the three first principal components extracted from the PCA
1151 of the elemental composition (PCe) of Sandhavn (factor scores plotted in Fig. 5).

1152

1153 Table SI3. Factor loadings from the PCA of the peat organic matter indicators (PCo) from
1154 Sandhavn (factor scores plotted in Fig. 7). The prefix 'b' relates to FTIR band widths.

Fig S11

[Click here to download high resolution image](#)

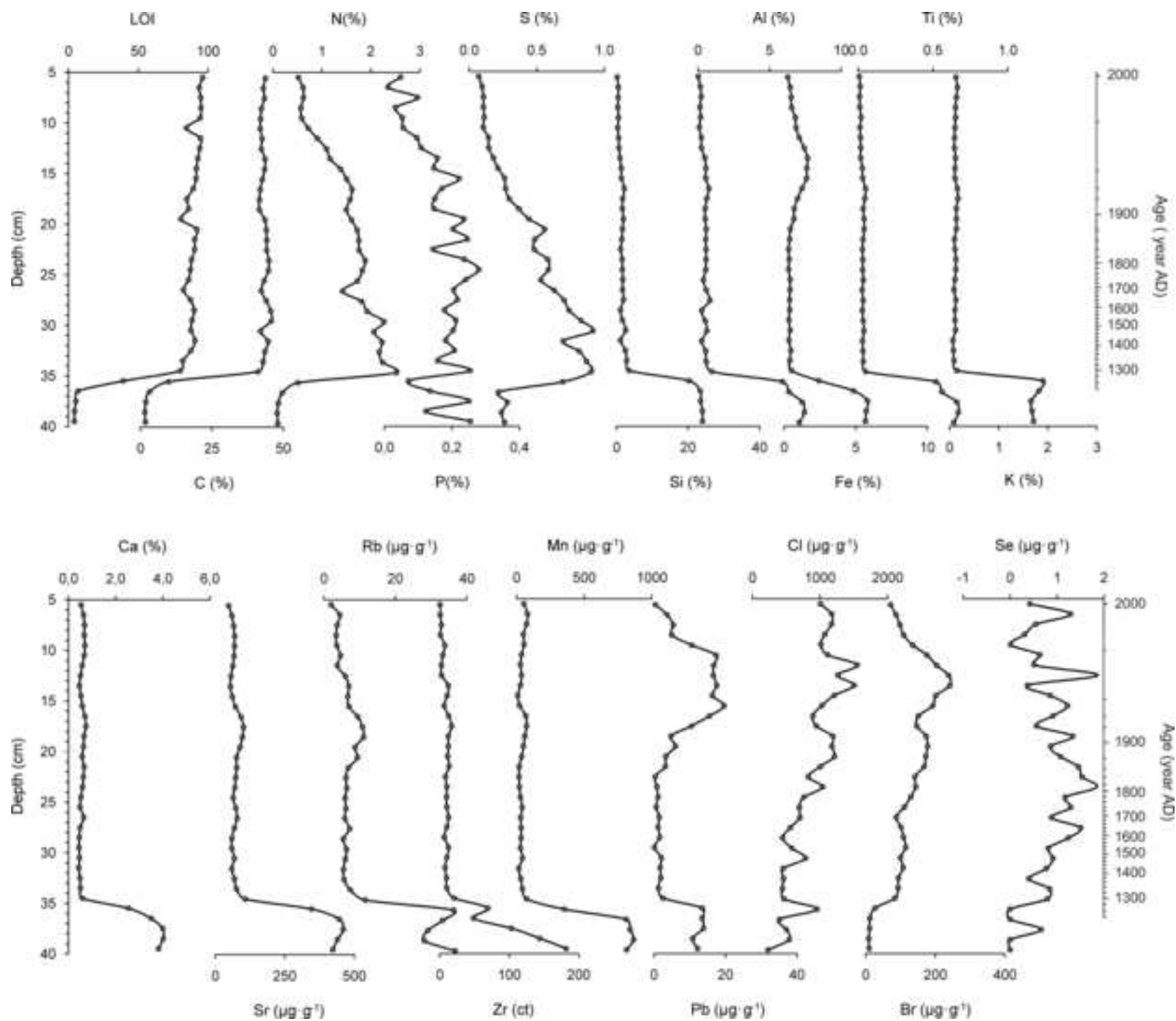


Table S11. Assignment and characterization of FTIR bands included in the principal components analysis of the peat organic matter properties from Sandhavn (plotted in Fig. 6).

Wavenumber (cm ⁻¹)	Assignment and Characterisation	References
3050-3030 (3051)	Aromatic CH stretching	(Guo and Bustin, 1998)
2922	Antisymmetric CH ₂ . Fats, wax, lipids	(Niemeyer et al., 1992; Coccozza et al., 2003)
2852	Symmetric CH ₂ ; Fats, wax, lipids	(Niemeyer et al., 1992; Coccozza et al., 2003)
1720	C=O stretch of COOH or COOR; Carboxylic acids, aromatic esters	(Niemeyer et al., 1992; Haberhauer et al., 1998)
1660	amides coming from preserved proteinaceous materials	(González et al., 2003)
1550	N-H in plane (amide II); Proteinaceous origin	(Ibarra et al., 1996; Zaccheo et al., 2002; González et al., 2003)
1514	Aromatic C=C stretching; Lignin/Phenolic backbone	(Coccozza et al., 2003)
1450-1371 (1450)	C-H deformations; Phenolic (lignin) and aliphatic structures	(Parker, 1971)
1420-1430 (1419)	Aromatic C=C ring stretching; lignin	(Guo and Bustin, 1998; González et al., 2003)
1250-1270 (1271)	Aromatic CO- and phenolic -OH stretching; lignin	(Guo and Bustin, 1998; González et al., 2003)
1080-1030 (1070, 1030)	Combination of C-O stretching and O-H deformation; Polysaccharides	(González et al., 2003; Grube et al., 2006)

Table S12: Factor loadings from the PCA of the elemental composition from Sandhavn (plotted in Fig. 5).

	PC1e	PC2e	PC3e
Ti	0.94	-0.09	0.10
Si	0.93	-0.22	-0.05
Zr	0.92	0.02	0.08
Al	0.91	0.02	0.04
Rb	0.86	0.20	0.33
N	0.83	-0.30	-0.39
P	0.78	-0.11	-0.32
Sr	0.74	0.02	0.59
S	0.69	-0.55	-0.41
LOI	-0.78	0.21	-0.07
Fe	0.01	0.94	-0.01
Br	-0.01	0.94	-0.09
Pb	-0.14	0.92	0.06
Cl	-0.45	0.71	0.32
K	0.11	0.04	0.87
Mn	-0.01	-0.21	0.84
Ca	-0.07	0.18	0.81
Se	0.21	0.00	-0.04
C	-0.15	-0.32	-0.54

Table S13. Factor loadings from the PCA of the peat organic matter indicators from Sandhavn (plotted in Fig. 7). The prefix 'b' relates to FTIR band widths.

	PC1o	PC2o	PC3o
b2852	0.97	0.18	0.04
b2922	0.94	0.24	0.11
b1514	0.89	0.43	-0.06
b1660	0.88	0.35	-0.21
b1550	0.87	0.30	-0.21
$\delta^{15}\text{N}$	0.84	-0.07	-0.10
b3051	0.76	-0.02	-0.53
C/N	-0.96	-0.05	0.03
$\delta^{13}\text{C}$	-0.65	-0.56	0.24
DPH	-0.53	0.07	0.16
b1450	0.18	0.97	0.01
b1271	0.27	0.89	0.22
b1419	-0.39	0.81	0.16
b1720	0.47	0.72	0.12
b1030	-0.12	0.11	0.97
b1070	-0.10	0.14	0.95

Figure 1
[Click here to download high resolution image](#)

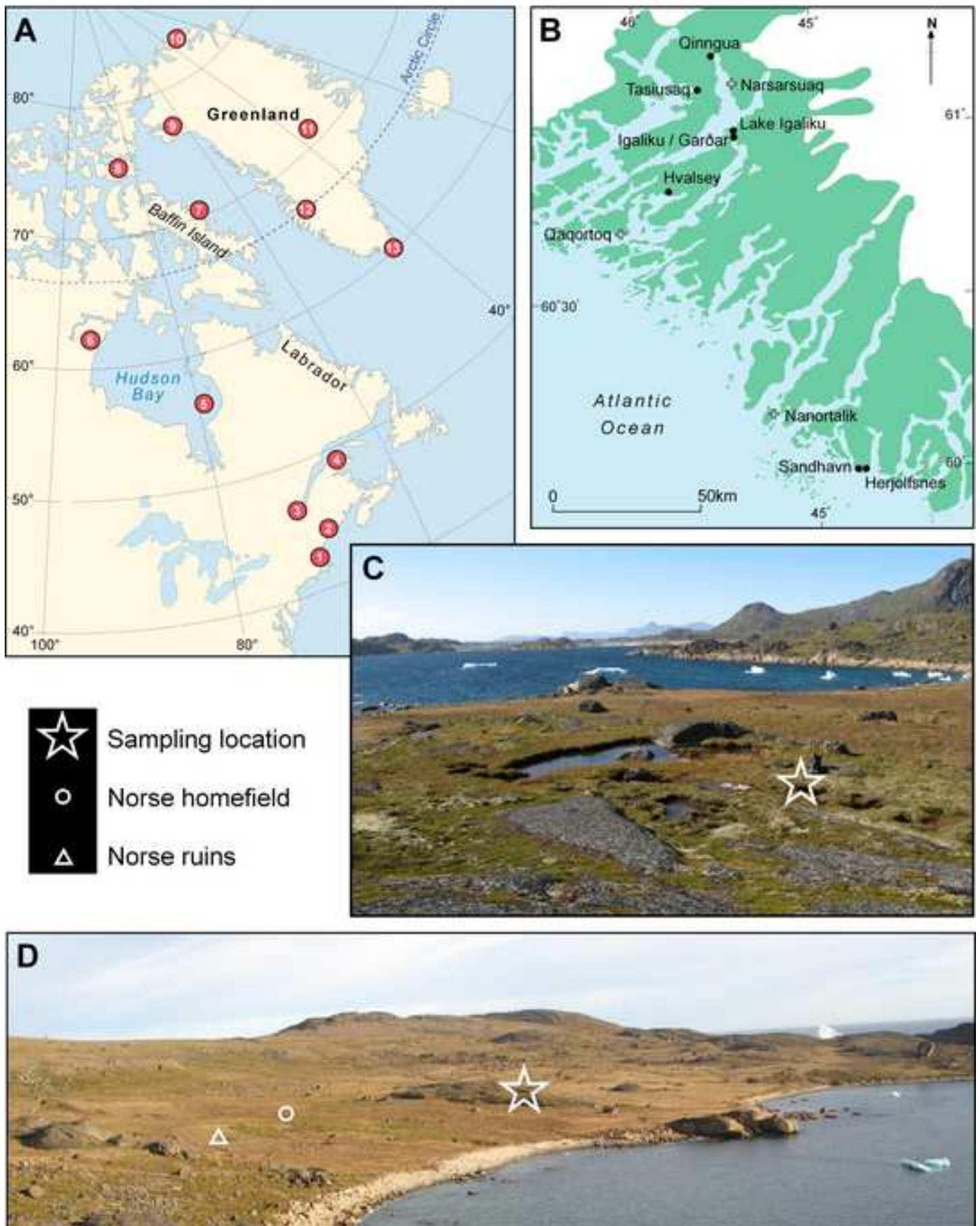


Figure 2
[Click here to download high resolution image](#)

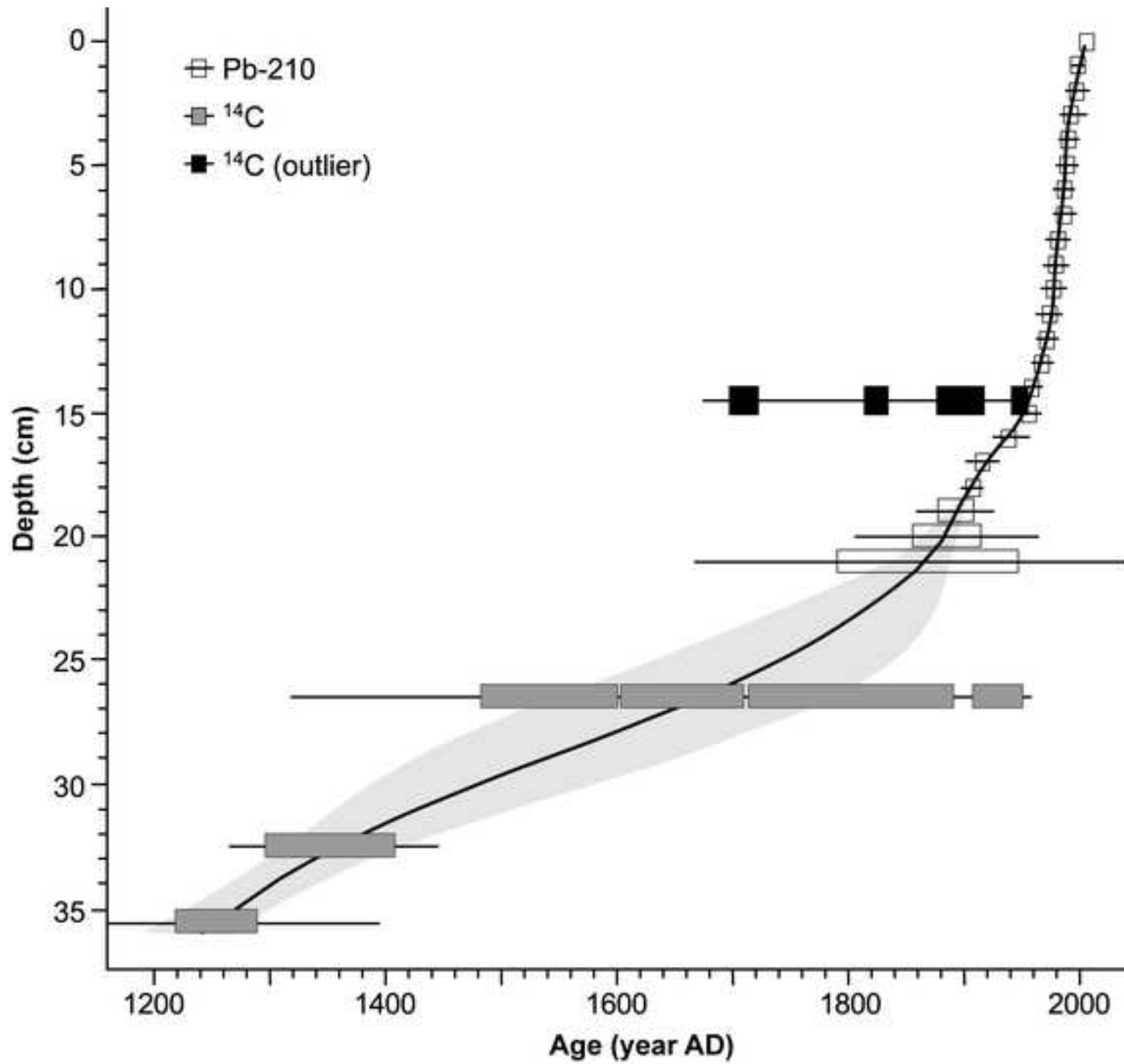


Figure 3 col
[Click here to download high resolution image](#)

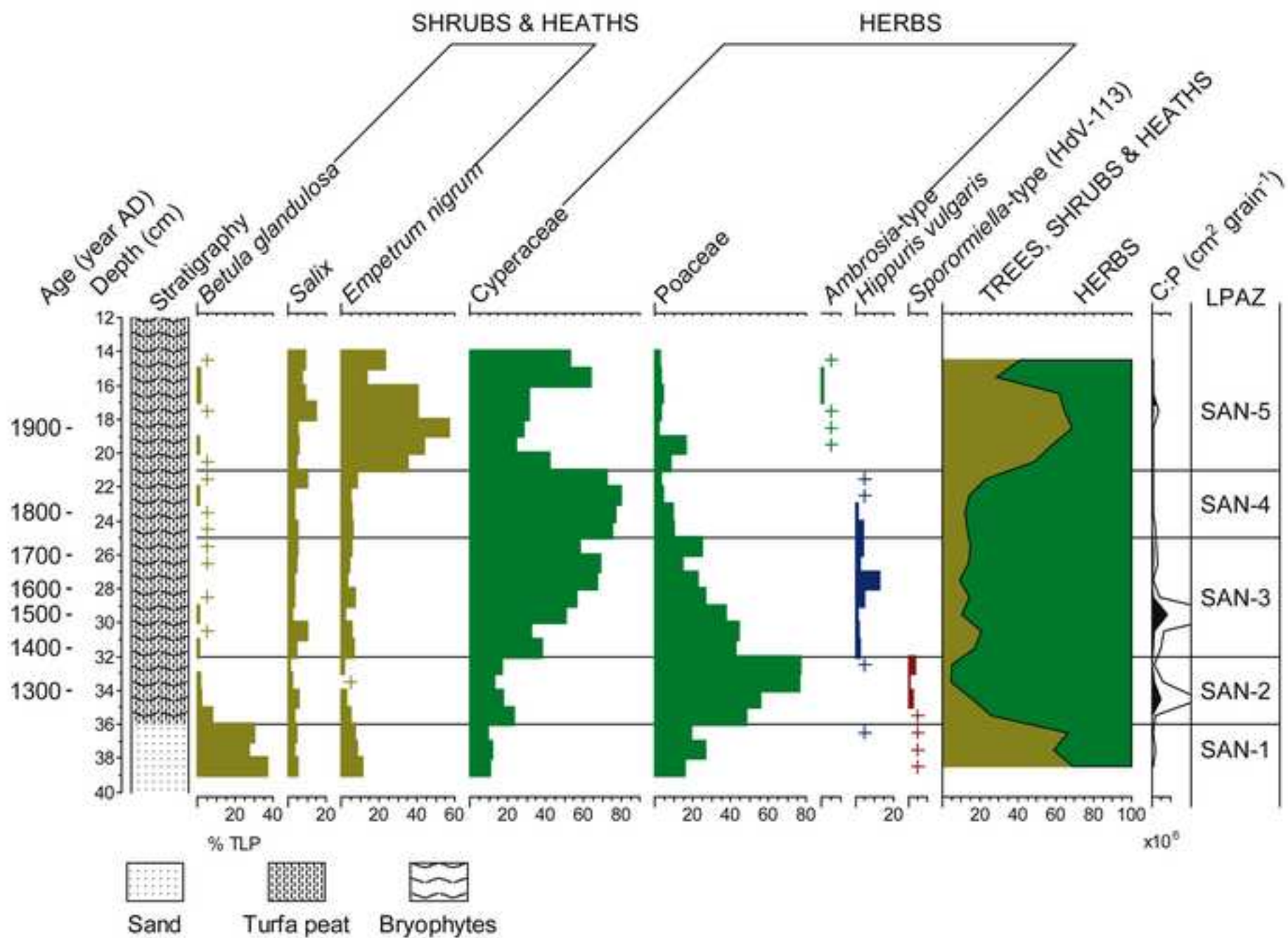


Figure 4
[Click here to download high resolution image](#)

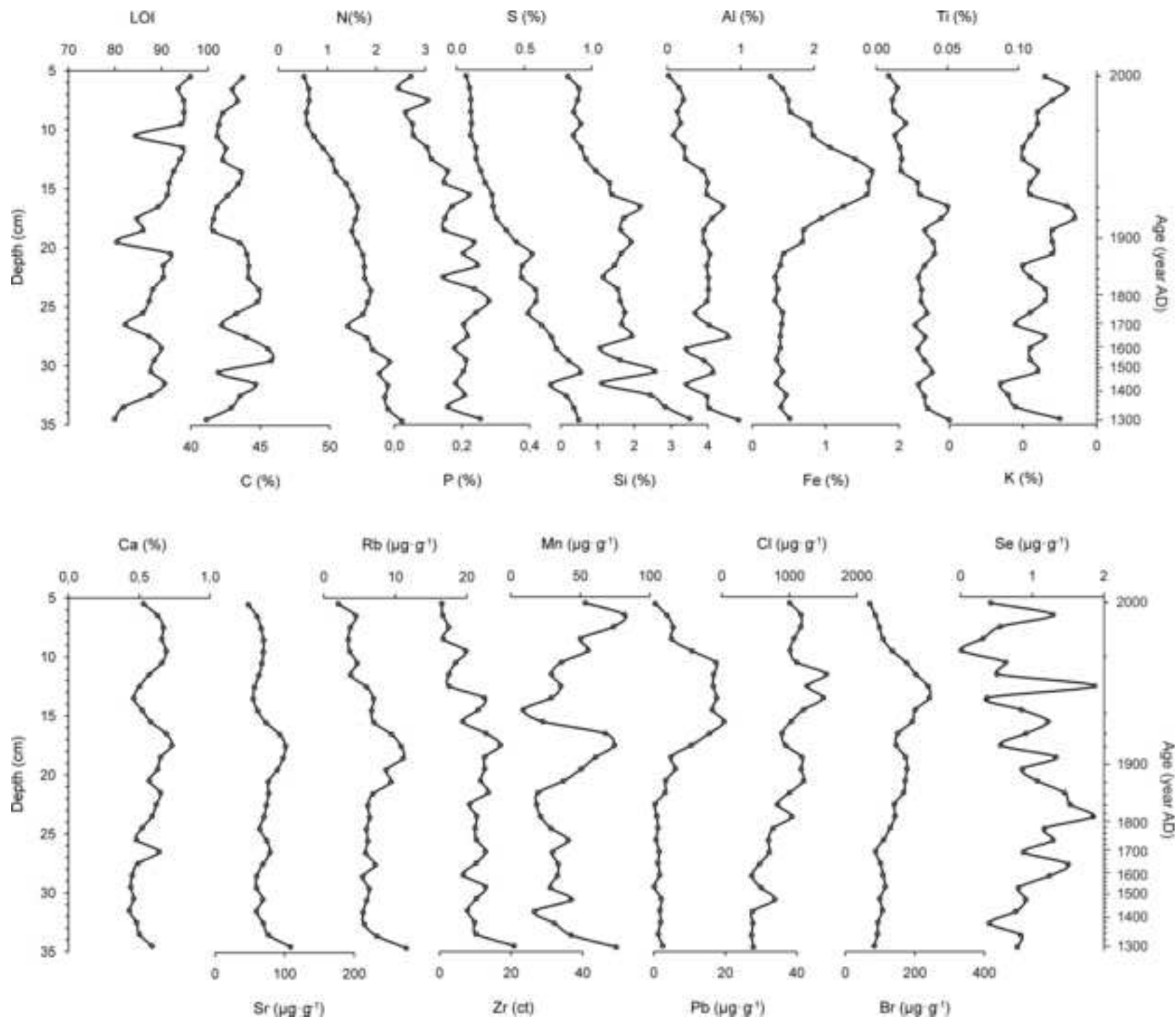


Figure 5
[Click here to download high resolution image](#)

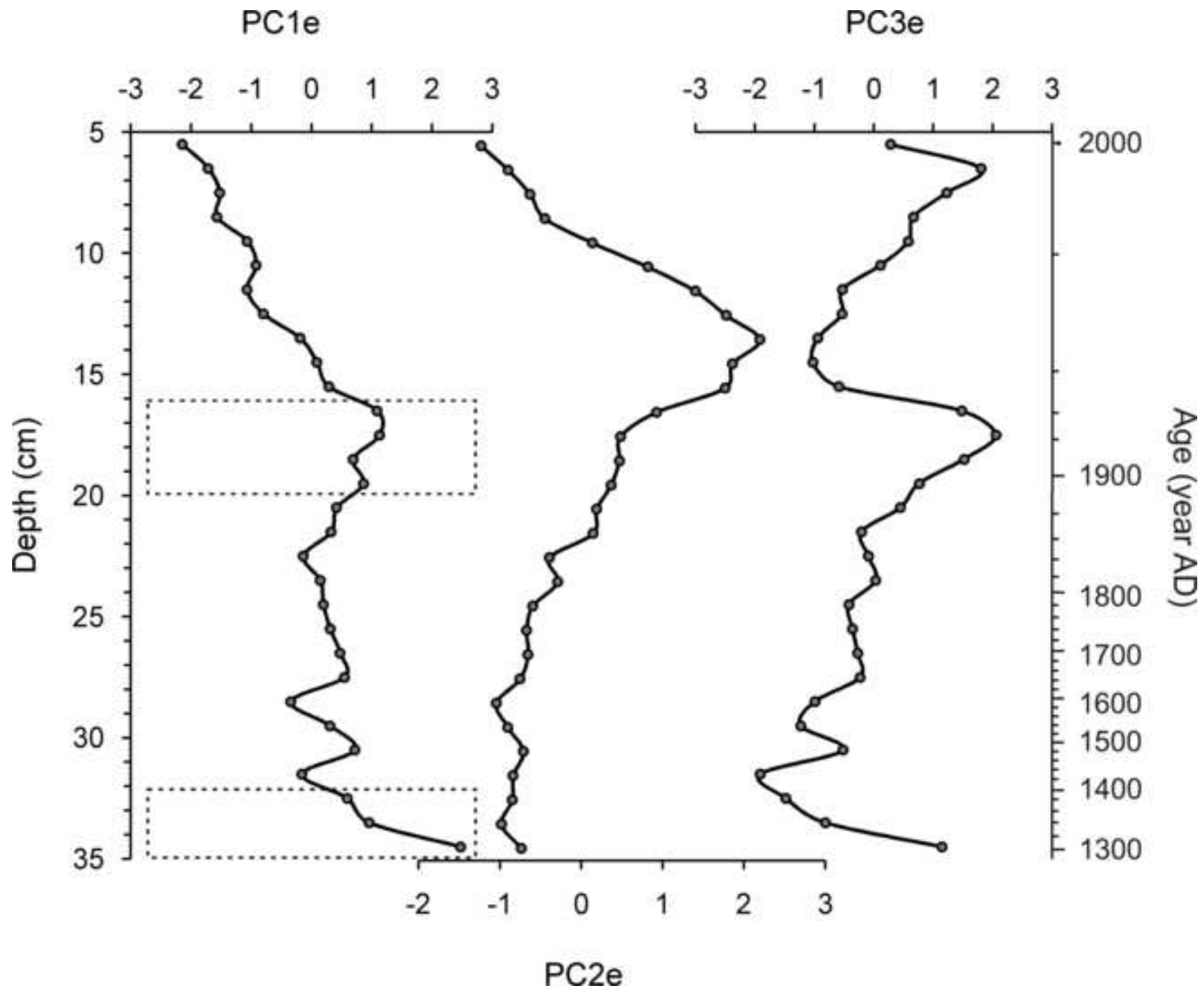


Figure 6
[Click here to download high resolution image](#)

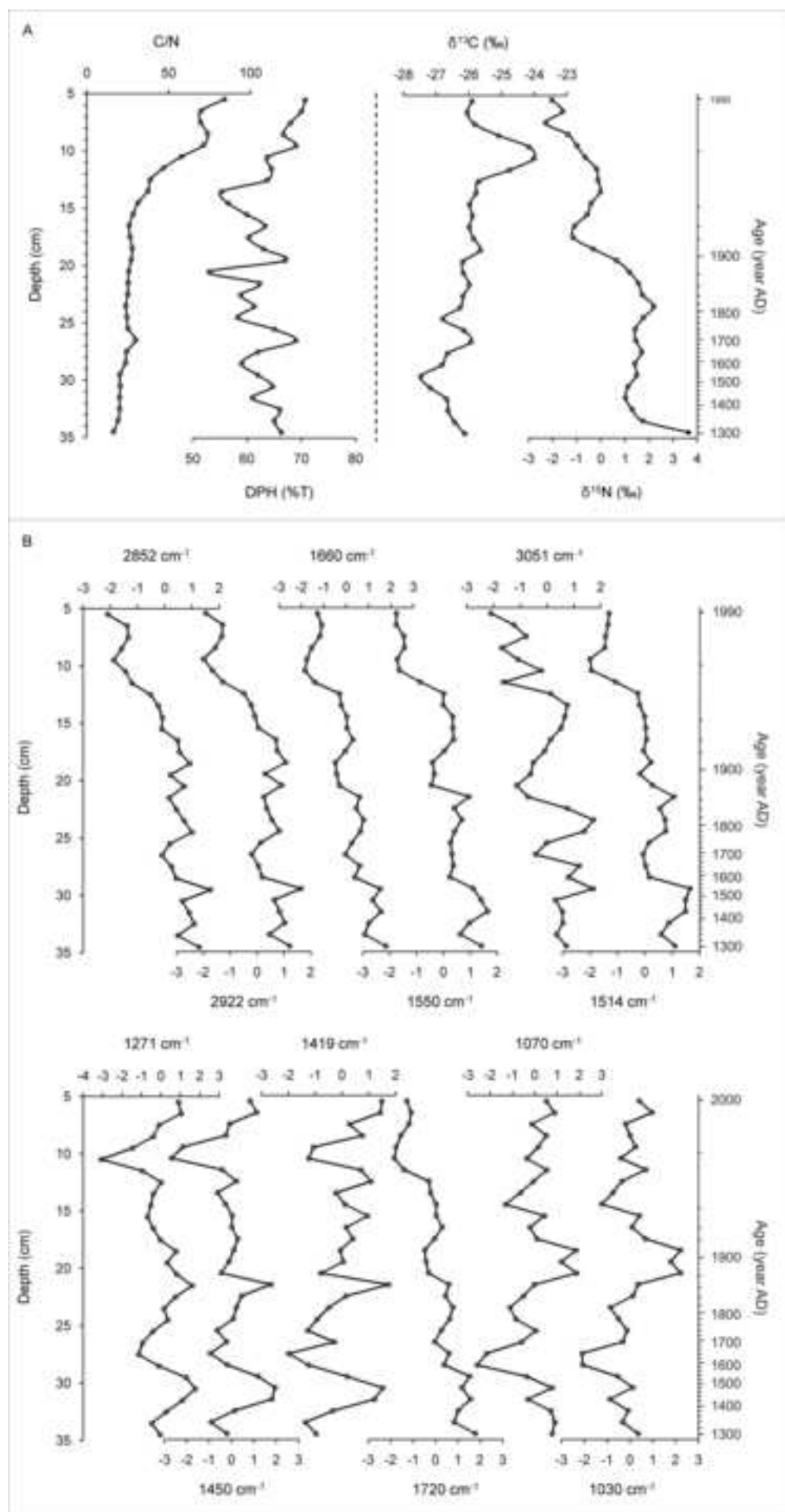


Figure 7
[Click here to download high resolution image](#)

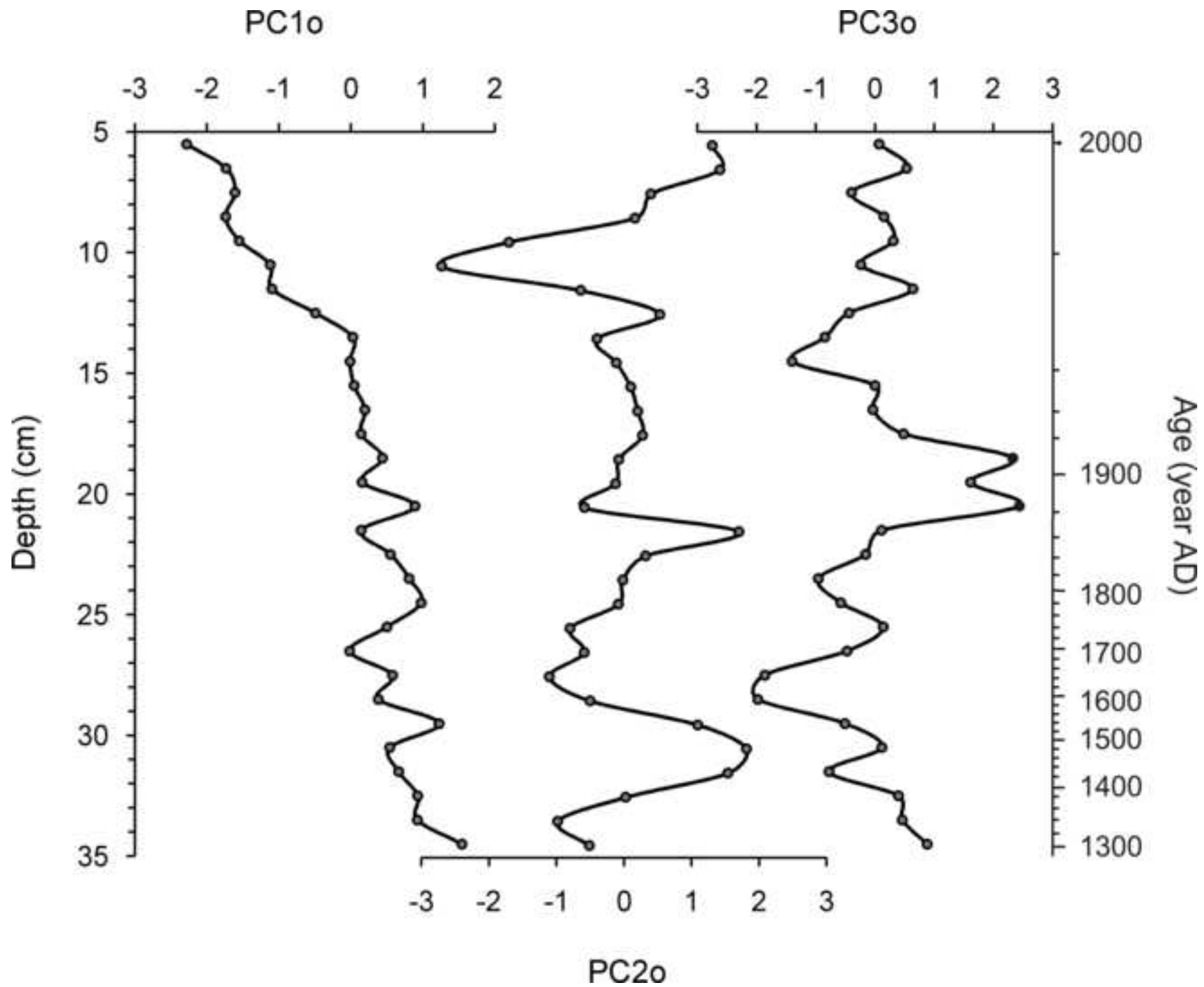


Figure 8
[Click here to download high resolution image](#)

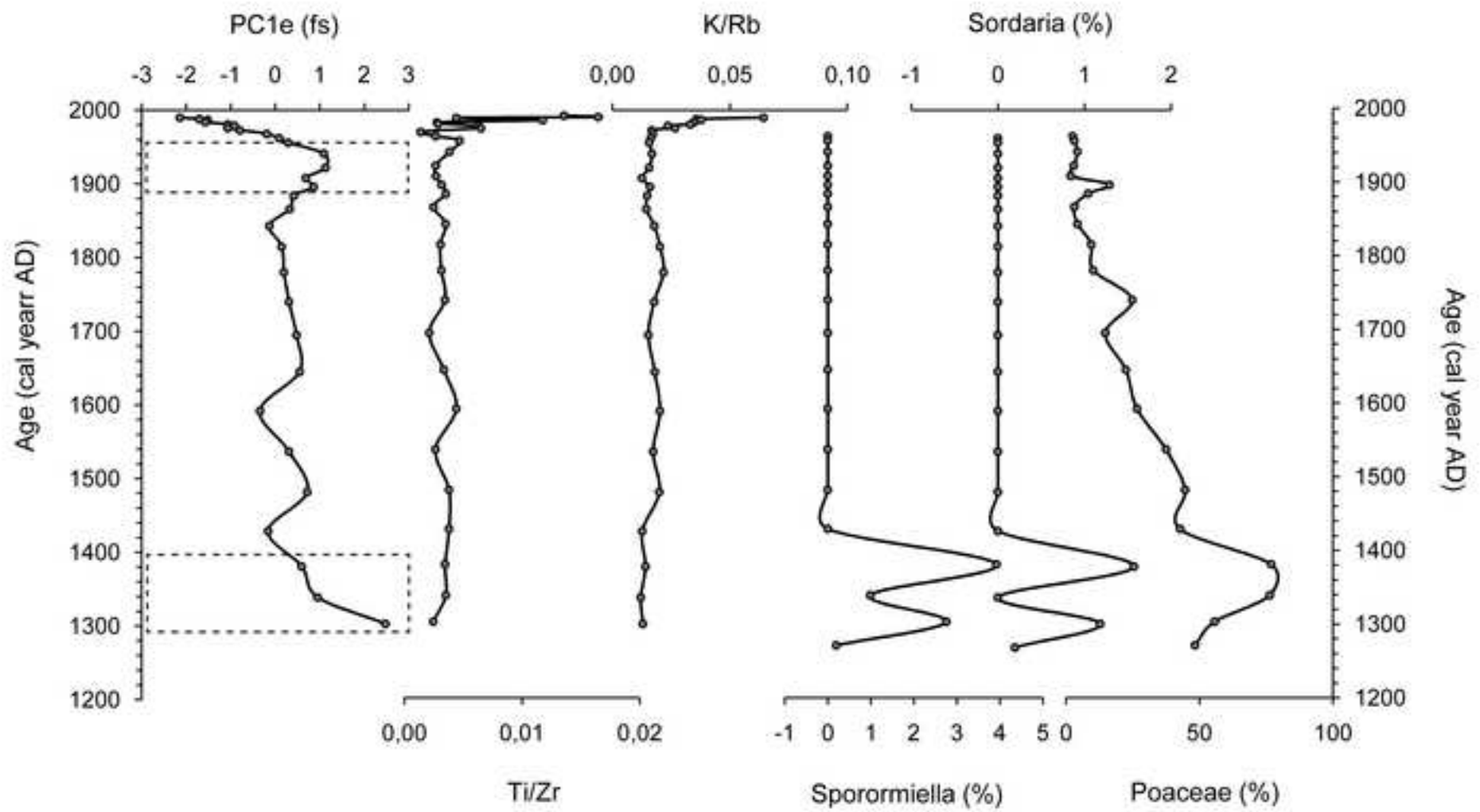


Figure 9

[Click here to download high resolution image](#)

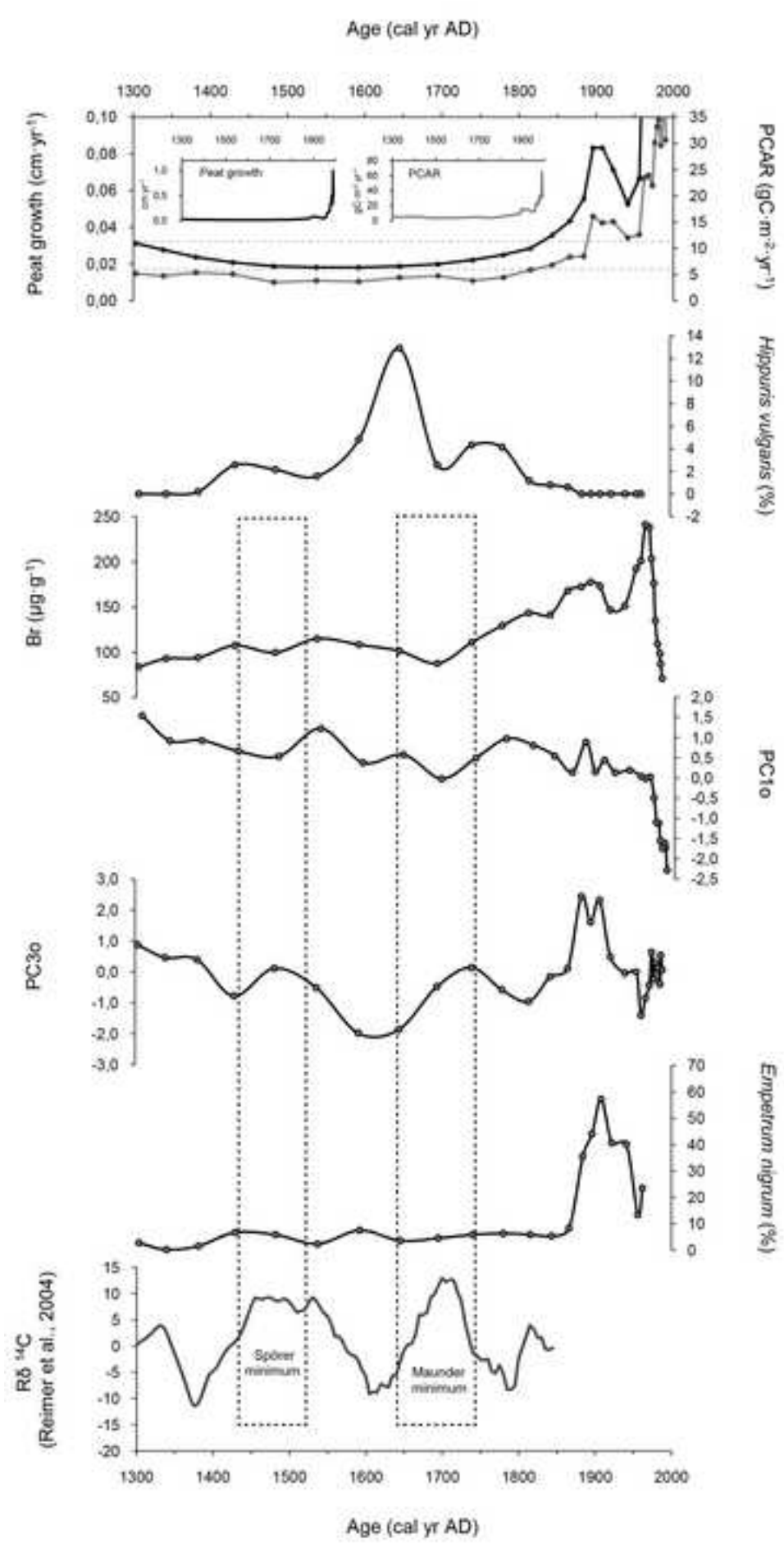


Figure 10
[Click here to download high resolution image](#)

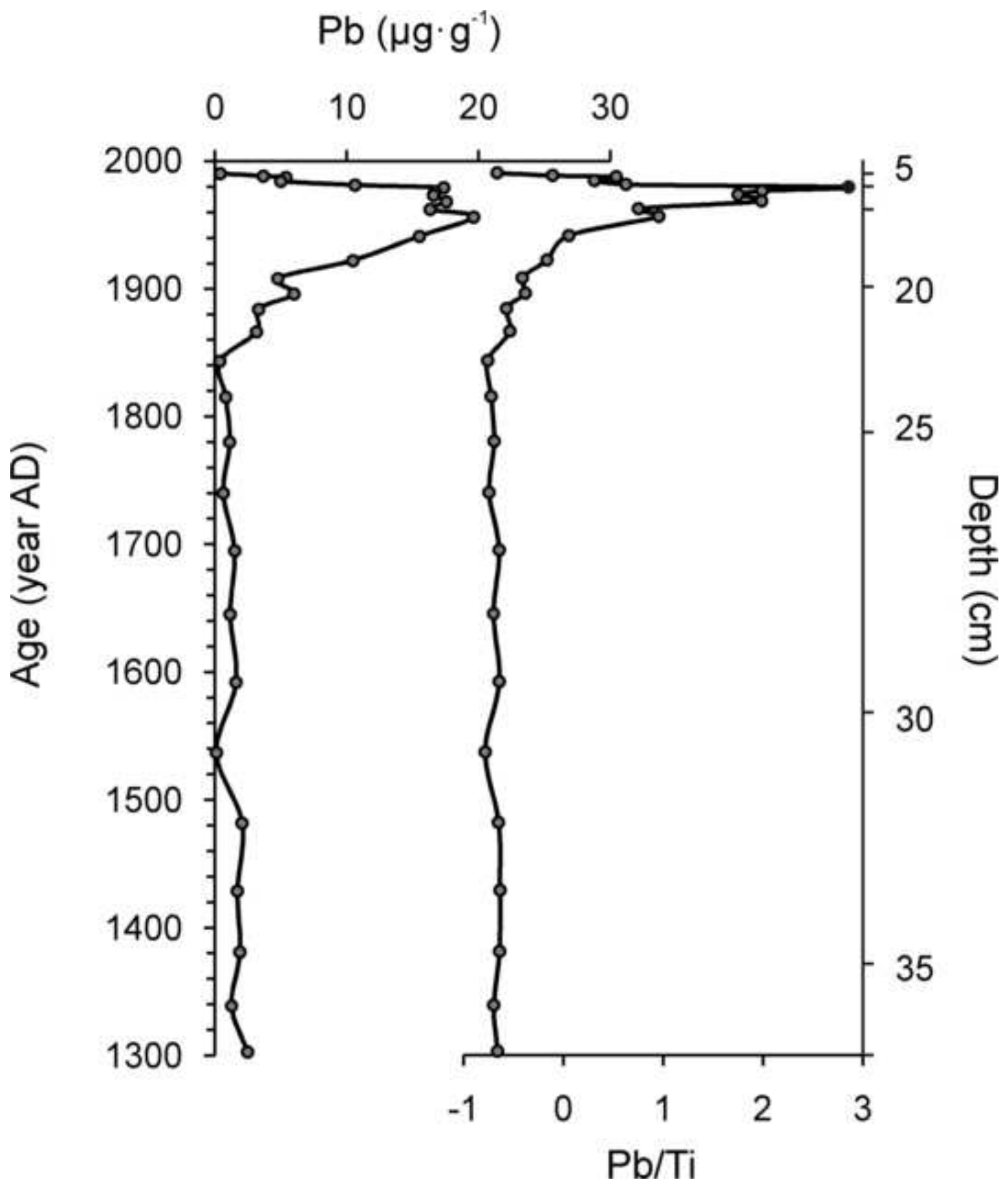


Table 1: Radiocarbon dates from Sandhavn. All measurements are AMS on bryophytes (*Dicranium*, *Drepanocladus*, *Hypnum*, *Hylocomium* and *Racomitrium* spp.). Calendar ranges are those used by the (*Clam*) age-depth model (Fig. 2) following calibration against the Intcal13 calibration curve (Reimer et al., 2013). See Golding et al. (2011) for a further discussion of the radiocarbon dates.

Depth (cm)	Lab code (SUERC-)	^{14}C age (BP)	AD range (2σ)	$\delta^{13}\text{C}$ (‰)
15-14	24657	0 ± 35	1698-1955	-23.6
27-26	24866	230 ± 90	1484-1953	-25.0
33-32	24658	600 ± 35	1297-1408	-25.6
36-35	24659	750 ± 35	1219-1290	-24.8